29

On the Chlorination Thermodynamics

Brocchi E. A. and Navarro R. C. S.
Pontifical Catholic University of Rio de Janeiro
Brazil

1. Introduction

Chlorination roasting has proven to be a very important industrial route and can be applied for different purposes. Firstly, the chlorination of some important minerals is a possible industrial process for producing and refining metals of considerable technological importance, such as titanium and zirconium. Also, the same principle is mentioned as a possible way of recovering rare earth from concentrates (Zang et al., 2004) and metals, of considerable economic value, from different industrial wastes, such as, tailings (Cechi et al., 2009), spent catalysts (Gabalah & Djona, 1995), slags (Brocchi & Moura, 2008) and fly ash (Murase et al., 1998). The chlorination processes are also presented as environmentally acceptable (Neff, 1995, Mackay, 1992).

In general terms the chlorination can be described as reaction between a starting material (mineral concentrate or industrial waste) with chlorine in order to produce some volatile chlorides, which can then be separated by, for example, selective condensation. The most desired chloride is purified and then used as a precursor in the production of either the pure metal (by reacting the chloride with magnesium) or its oxide (by oxidation of the chloride).

The chlorination reaction has been studied on respect of many metal oxides (Micco et. al., 2011; Gaviria & Bohe, 2010; Esquivel et al., 2003; Oheda et al., 2002) as this type of compound is the most common in the mentioned starting materials. Although some basic thermodynamic data is enclosed in these works, most of them are related to kinetics aspects of the gas – solid reactions. However, it is clear that the understanding of the equilibrium conditions, as predicted by classical thermodynamics, of a particular oxide reaction with chlorine can give strong support for both the control and optimization of the process. In this context, the impact of industrial operational variables over the chlorination efficiency, such as the reaction temperature and the reactors atmosphere composition, can be theoretically appreciated and then quantitatively predicted. On that sense, some important works have been totally devoted to the thermodynamics of the chlorination and became classical references on the subject (Kellog, 1950; Patel & Jere, 1960; Pilgrim & Ingraham, 1967; Sano & Belton, 1980).

Originally, the approach applied for the study of chemical equilibrium studies was based exclusively on ΔG_r^o x T and predominance diagrams. Nowadays, however, advances in computational thermodynamics enabled the development of softwares that can perform more complex calculations. This approach, together with the one accomplished by simpler techniques, converge to a better understanding of the intimate nature of the equilibrium states for the reaction system of interest. Therefore, it is understood that the time has come

for a review on chlorination thermodynamics which can combine its basic aspects with a now available new kind of approach.

The present chapter will first focus on the thermodynamic basis necessary for understanding the nature of the equilibrium states achievable through chlorination reactions of metallic oxides. Possible ways of graphically representing the equilibrium conditions are discussed and compared. Moreover, the chlorination of V_2O_5, both in the absence as with the presence of graphite will be considered. The need of such reducing agent is clearly explained and discussed. Finally, the equilibrium conditions are appreciated through the construction of graphics with different levels of complexity, beginning with the well known ΔG_r^o x T diagrams, and ending with gas phase speciation diagrams, rigorously calculated through the minimization of the total Gibbs energy of the system.

2. Chemical reaction equilibria

The equilibrium state achieved by a system where a group of chemical reactions take place simultaneously can be entirely modeled and predicted by applying the principles of classical thermodynamics.

Supposing that we want to react some solid transition metal oxide, say M_2O_5, with gaseous Cl_2. Lets consider for simplicity that the reaction can result in the formation of only one gaseous chlorinated specie, say MCl_5. The transformation is represented by the following equation:

$$M_2O_5(s) + 5Cl_2(g) \rightarrow 2MCl_5(g) + \frac{5}{2}O_2(g) \tag{1}$$

In this system there are only two phases, the pure solid oxide M_2O_5 and a gas phase, whose composition is characterized by definite proportions of Cl_2, O_2, and MCl_5. If temperature, total pressure, and the total molar amounts of O, Cl, and M are fixed, the chemical equilibrium is calculated by finding the global minimum of the total Gibbs energy of the system (Robert, 1993).

$$G = n^s_{M_2O_5} g^s_{M_2O_5} + G^g \tag{2}$$

Where $g^s_{M_2O_5}$ represents the molar Gibbs energy of pure solid M_2O_5 at reaction's temperature and total pressure, $n^s_{M_2O_5}$ the number of moles of M_2O_5 and G^g the molar Gibbs energy of the gaseous phase, which can be computed through the knowledge of the *chemical potential* of all molecular species present ($\mu^g_{Cl_2}$, $\mu^g_{O_2}$, $\mu^g_{MCl_5}$):

$$G^g = n^g_{Cl_2}\mu^g_{Cl_2} + n^g_{O_2}\mu^g_{O_2} + n^g_{MCl_5}\mu^g_{MCl_5}$$
$$\mu^g_{Cl_2} = \left(\frac{\partial G^g}{\partial n^g_{Cl_2}}\right)_{T,P,n_{O_2},n_{MCl5}} \tag{3}$$

The minimization of function (2) requires that for the restrictions imposed to the system, the first order differential of *G* must be equal to zero. By fixing the reaction temperature (*T*) and pressure (*P*) and total amount of each one of the elements, this condition can be written according to equation (4) (Robert, 1993).

$$dG_{T,P,n_O,n_{Cl},n_M} = 0$$
$$dG = g^s_{M_2O_5} dn_{M_2O_5} + \mu^g_{Cl_2} dn_{Cl_2} + \mu^g_{O_2} dn_{O_2} + \mu^g_{MCl_5} dn_{MCl_5} \quad (4)$$
$$g^s_{M_2O_5} dn_{M_2O_5} + \mu^g_{Cl_2} dn_{Cl_2} + \mu^g_{O_2} dn_{O_2} + \mu^g_{MCl_5} dn_{MCl_5} = 0$$

The development of the chlorination reaction can be followed through introduction of a reaction coordinate called *degree of reaction* (ε),whose first differential is computed by the ratio of its molar content variation of each specie participating in the reaction and the stoichiometric coefficient(Eq. 1).

$$d\varepsilon = \frac{dn_{Cl_2}}{(-5)} = \frac{dn_{M_2O_5}}{(-1)} = \frac{dn_{O_2}}{(+5/2)} = \frac{dn_{MCl_5}}{(+2)} \quad (5)$$

The numbers inside the parenthesis in the denominators of the fractions contained in equation (5) are the stoichiometric coefficient of each specie multiplied by "-1" if it is represented as a reactant, or "+1" if it is a product. The equilibrium condition (Eq. 4) can now be rewritten in the following mathematical form:

$$-g^s_{M_2O_5} d\varepsilon - 5\mu^g_{Cl_2} d\varepsilon + \frac{5}{2}\mu^g_{O_2} d\varepsilon + 2\mu^g_{MCl_5} d\varepsilon = 0$$
$$\left(-g^s_{M_2O_5} - 5\mu^g_{Cl_2} + \frac{5}{2}\mu^g_{O_2} + 2\mu^g_{MCl_5}\right) d\varepsilon = 0 \quad (6)$$

At the desired equilibrium state the condition defined by Eq. (6) must be valid for all possible values of the differential $d\varepsilon$. This can only be accomplished if the term inside the parenthesis is equal to zero. This last condition is the simplest mathematical representation for the chemical equilibrium associated with reaction (1).

$$-g^s_{M_2O_5} - 5\mu^g_{Cl_2} + \frac{5}{2}\mu^g_{O_2} + 2\mu^g_{MCl_5} = 0 \quad (7)$$

The chemical potentials can be computed through knowledge of the molar Gibbs energy of each pure specie in the gas phase, and its chemical activity. For the chloride MCl_5, for example, the following function can be used (Robert, 1993):

$$\mu^g_{MCl_5} = g^g_{MCl_5} + RT \ln a^g_{MCl_5} \quad (8)$$

Where $a^g_{MCl_5}$ represents the chemical activity of the component MCl_5 in the gas phase. By introducing equations analogous to Eq. (8) for all components of the gas phase, Eq. (7) can be rewritten according to Eq. (9). There, the activity of M_2O_5 is not present in the term located at the left hand side because, as this oxide is assumed to be pure, its activity must be equal to one (Robert, 1993).

$$\ln\left(\frac{a^2_{MCl_5} a^{5/2}_{O_2}}{a^5_{Cl_2}}\right) = -\frac{\left(2g^g_{MCl_5} + \frac{5}{2}g^g_{O_2} - 5g^g_{Cl_2} - g^s_{M_2O_5}\right)}{RT} = -\frac{\Delta G_r}{RT} \quad (9)$$

The numerator of the right side of Eq. (9) represents the molar Gibbs energy of reaction (1). It involves only the molar Gibbs energies of the species participating in the reaction as pure substances, at T and P established in the reactor. The molar Gibbs energy of a pure component is only a function of T and P (Eq. 10), so the same must be valid for the reactions Gibbs energy (Robert, 1993).

$$dg(T,P) = -sdT + vdP \tag{10}$$

Where s and v denote respectively the molar entropy and molar volume of the material, which for a pure substance are themselves only a function of T and P.

It is a common practice in treating reactions involving gaseous species to calculate the Gibbs energy of reaction not at the total pressure prevailing inside the reactor, but to fix it at 1 atm. This is in fact a reference pressure, and can assume any suitable value we desire. The molar Gibbs energy of reaction is in this case referred to as the *standard molar Gibbs energy of reaction*. According to this definition, the standard Gibbs energy of reaction must depend only on the reactor's temperature.

By assuming that the total pressure inside the reactor (P) is low enough for neglecting the effect of the interactions among the species present in the gas phase, Eq. (9) can be rewritten in the following form:

$$\frac{P_{MCl_5}{}^2 P_{O_2}{}^{5/2}}{P_{Cl_2}{}^5} = \exp\left(-\frac{\left(2g^g_{MCl_5} + \frac{5}{2}g^g_{O_2} - 5g^g_{Cl_2} - g^s_{M_2O_5}\right)}{RT}\right) \tag{11}$$

The activities were calculated as the ratio of the partial pressure of each component and the reference pressure chosen (P = 1 atm). This proposal is based on the thermodynamic description of an ideal gas (Robert, 1993). For MCl_5, for example, the chemical activity is calculated as follows:

$$a_{MCl_5} = \frac{P_{MCl_5}}{1} = P_{MCl_5} = x^g_{MCl_5} P \tag{12}$$

Where $x^g_{MCl_5}$ stands for the mol fraction of MCl_5 in the gas phase. Similar relations hold for the other species present in the reactor atmosphere. The activity is then expressed as the product of the mol fraction of the specie and the total pressure exerted by the gaseous solution.

The right hand side of Eq. (11) defines the equilibrium constant (K) of the reaction in question. This quantity can be calculated as follows:

$$K = \exp\left(-\frac{\Delta G^o_r}{RT}\right) \tag{13}$$

The symbol "o" is used to denote that The molar reaction Gibbs energy (ΔG^o_r) is calculated at a reference pressure of 1 atm.

At this point, three possible situations arise. If the standard molar Gibbs energy of the reaction is negative, then $K > 1$. If it is positive, $K < 1$ and if it is equal to zero $K = 1$. The first

situation defines a process where in the achieved equilibrium state, the atmosphere tends to be richer in the desired products. The second situation characterizes a reaction where the reactants are present in higher concentration in equilibrium. Finally, the third possibility defines the situation where products and reactants are present in amounts of the same order of magnitude.

2.1 Thermodynamic driving force and ΔG_r^o vs. T diagrams

Equation (6) can be used to formulate a mathematical definition of the thermodynamic driving force for a chlorination reaction. If the reaction proceeds in the desired direction, then $d\varepsilon$ must be positive. Based on the fact that by fixing T, P, n(O), n(Cl), and n(M) the total Gibbs energy of the system is minimum at the equilibrium, the reaction will develop in the direction of the final equilibrium state, if and only if, the value of G reduces, or in other words, the following inequality must then be valid:

$$-g^{s}_{M_2O_5} - 5\mu^{g}_{Cl_2} + \frac{5}{2}\mu^{g}_{O_2} + 2\mu^{g}_{MCl_5} < 0 \tag{14}$$

The left hand side of inequality (14) defines the thermodynamic driving force of the reaction ($\Delta\mu_r$).

$$\Delta\mu_r = -g^{s}_{M_2O_5} - 5\mu^{g}_{Cl_2} + \frac{5}{2}\mu^{g}_{O_2} + 2\mu^{g}_{MCl_5} \tag{15}$$

If $\Delta\mu_r$ is negative, classical thermodynamics says that the process will develop in the direction of obtaining the desired products. However, a positive value is indicative that the reaction will develop in the opposite direction. In this case, the formed products react to regenerate the reactants. By using the mathematical expression for the chemical potentials (Eq. 8), it is possible to rewrite the driving force in a more familiar way:

$$\Delta\mu_r = \Delta G_r^o + RT\ln\left(\frac{P^2_{MCl_5}P^{5/2}_{O_2}}{P^5_{Cl_2}}\right) = \Delta G_r^o + RT\ln Q \tag{16}$$

According to Eq. (16), the ratio involving the partial pressure of the components defines the so called *reaction coefficient* (Q). This parameter can be specified in a given experiment by injecting a gas with the desired proportion of O_2 and Cl_2. The partial pressure of MCl_5, on the other hand, would then be near zero, as after the formation of each species, the fluxing gas removes it from the atmosphere in the neighborhood of the sample.

At a fixed temperature and depending on the value of Q and the standard molar Gibbs energy of the reaction considered, the driving force can be positive, negative or zero. In the last case the reaction ceases and the equilibrium condition is achieved. It is important to note, however, that by only evaluating the reactions Gibbs energy one is not in condition to predict the reaction path followed, then even for positive values of ΔG_r^o, it is possible to find a value Q that makes the driving force negative. This is a usual situation faced in industry, where the desired equilibrium is forced by continuously injecting reactants, or removing products. In all cases, however, for computing reaction driving forces it is vital to know the temperature dependence of the reaction Gibbs energy.

2.1.1 Thermodynamic basis for the construction of ΔG_r^o x T diagrams

To construct the ΔG_r^o x T diagram of a particular reaction we must be able to compute its standard Gibbs energy in the whole temperature range spanned by the diagram.

$$\begin{gathered}\Delta G_r^o = \Delta H_r^o - T\Delta S_r^o \\ \Delta H_r^o = \Delta H_{298} + \int_{298.15\ K}^{T} \Delta C_P^o dT \\ \Delta S_r^o = \Delta S_{298} + \int_{298.15\ K}^{T} \frac{\Delta C_P^o}{T} dT \\ \Delta C_P^o = \frac{d\Delta H_r^o}{dT} = 2C_{P,MCl_5}^{o,g} + \frac{5}{2}C_{P,O_2}^{g} - 5C_{P,Cl_2}^{g} - C_{P,M_2O_5}^{s} \\ \Delta H_{298} = 2H_{298,\,MCl_5}^{o} + \frac{5}{2}H_{298,O_2}^{g} - 5H_{298,Cl_2}^{g} - H_{298,M_2O_5}^{s} \\ \Delta S_{298} = 2S_{298,\,MCl_5}^{o} + \frac{5}{2}S_{298,O_2}^{g} - 5S_{298,Cl_2}^{g} - S_{298,M_2O_5}^{s}\end{gathered} \tag{17}$$

For accomplishing this task one needs a mathematical model for the molar standard heat capacity at constant pressure, valid for each participating substance for T varying between 298.15 K and the final desired temperature, its molar enthalpy of formation (H_{298}^o) and its molar entropy of formation (S_{298}^o)at 298.15 K

For the most gas – solid reactions both the molar standard enthalpy (ΔH_r^o) and entropy of reaction (ΔS_r^o) do not depend strongly on temperature, as far no phase transformation among the reactants and or products are present in the considered temperature range. So, the observed behavior is usually described by a line (Fig. 1), whose angular coefficient gives us a measurement of ΔS_r^o and ΔH_r^o is defined by the linear coefficient.

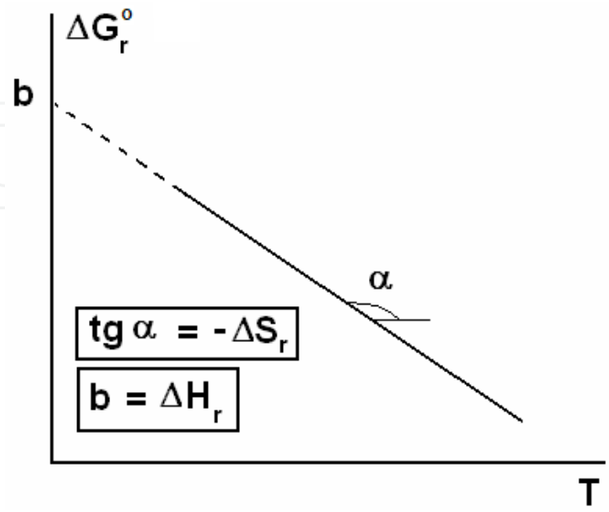

Fig. 1. Hypothetical ΔG_r^o x T diagram

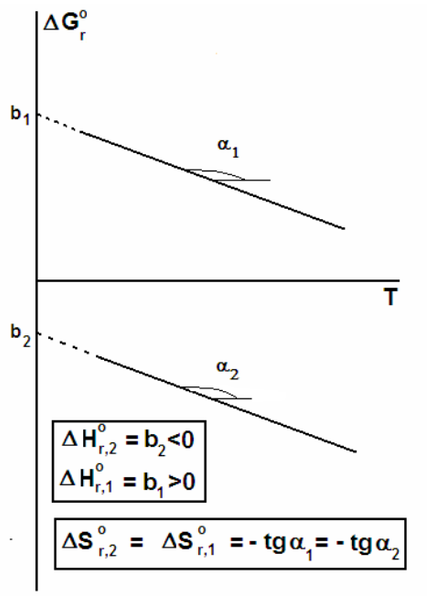

Fig. 2. Endothermic and exothermic reactions

Further, for a reaction defined by Eq. (1) the number of moles of gaseous products is higher than the number of moles of gaseous reactants, which, based on the ideal gas model, is indicative that the chlorination leads to a state of grater disorder, or greater entropy. In this particular case then, the straight line must have negative linear coefficient ($-\Delta S_r^o < 0$), as depicted in the graph of Figure (1).

The same can not be said about the molar reaction enthalpy. In principle the chlorination reaction can lead to an evolution of heat (exothermic process, then $\Delta H_r^o < 0$) or absorption of heat (endothermic process, then $\Delta H_r^o > 0$). In the first case the linear coefficient is positive, but in the later it is negative. Hypothetical cases are presented in Fig. (2) for the chlorination of two oxides, which react according to equations identical to Eq. (1). The same molar reaction entropy is observed, but for one oxide the molar enthalpy is positive, and for the other it is negative.

Finally, it is worthwhile to mention that for some reactions the angular coefficient of the straight line can change at a particular temperature value. This can happen due to a phase transformation associated with either a reactant or a product. In the case of the reaction (1), only the oxide M_2O_5 can experience some phase transformation (melting, sublimation, or ebullition), all of them associated with an increase in the molar enthalpy of the phase. According to classical thermodynamics, the molar entropy of the compound must also increase (Robert, 1993).

$$\Delta S_t = \frac{\Delta H_t}{T_t} \tag{18}$$

Where ΔS_t, ΔH_t and T_t represent respectively, the molar entropy, molar enthalpy and temperature of the phase transformation in question. So, to include the effect for melting of M_2O_5 at a temperature T_t, the molar reaction enthalpy and entropy must be modified as follows.

$$\Delta H_r^o = \int_{298.15}^{T_t} \Delta C_P^o dT - \Delta H_{t,M_2O_5} + \int_{T_t}^{T} \Delta C_P^o dT$$
$$\Delta S_r^o = \int_{298.15}^{T_t} \frac{\Delta C_P^o}{T} dT - \frac{\Delta H_{t,M_2O_5}}{T_t} + \int_{T_t}^{T} \frac{\Delta C_P^o}{T} dT \quad (19)$$

It should be observed that the molar entropy and enthalpy associated with the phase transition experienced by the oxide M_2O_5 were multiplied by its stoichiometric number "-1", which explains the minus sign present in both relations of Eq. (19).

An analogous procedure can be applied if other phase transition phenomena take place. One must only be aware that the mathematical description for the molar reaction heat capacity at constant pressure (ΔC_P^o) must be modified by substituting the heat capacity of solid M_2O_5 for a model associated with the most stable phase in each particular temperature range. If, for example, in the temperature range of interest M_2O_5 melts at T_t, for $T > T_t$, the molar heat capacity of solid M_2O_5 must be substituted for the model associated with the liquid state (Eq. 20).

$$\Delta C_P^o = 2C_{P,MCl_5}^{o,g} + \frac{5}{2}C_{P,O_2}^{g} - 5C_{P,Cl_2}^{g} - C_{P,M_2O_5}^{s} \quad (T < T_t)$$
$$\Delta C_P^o = 2C_{P,MCl_5}^{o,g} + \frac{5}{2}C_{P,O_2}^{g} - 5C_{P,Cl_2}^{g} - C_{P,M_2O_5}^{l} \quad (T > T_t) \quad (20)$$

The effect of a phase transition over the geometric nature of the ΔG_r^o x T curve can be directly seen. The melting of M_2O_5 makes it's molar enthalpy and entropy higher. According to Eq. (19), such effects would make the molar reaction enthalpy and entropy lower. So the curve should experience a decrease in its first order derivative at the melting temperature (Figure 3).

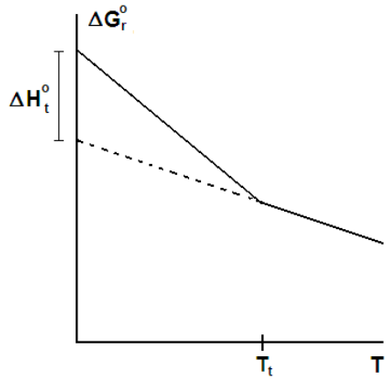

Fig. 3. Effect of M_2O_5 melting over the ΔG_r^o x T diagram

Based on the definition of the reaction Gibbs energy (Eq. 17), similar transitions involving a product would produce an opposite effect. The reaction Gibbs energy would in these cases dislocate to more negative values. In all cases, though, the magnitude of the deviation is proportional to the magnitude of the molar enthalpy associated with the particular transition observed. The effect increases in the following order: melting, ebullition and sublimation.

2.2 Multiple reactions

In many situations the reaction of a metallic oxide with Cl_2 leads to the formation of a family of chlorinated species. In these cases, multiple reactions take place. In the present section three methods will be described for treating this sort of situation, the first of them is of qualitative nature, the second semi-qualitative, and the third a rigorous one, that reproduces the equilibrium conditions quantitatively.

The first method consists in calculating ΔG_r^o x T diagrams for each reaction in the temperature range of interest. The reaction with the lower molar Gibbs energy must have a greater thermodynamic driving force. The second method involves the solution of the equilibrium equations independently for each reaction, and plotting on the same space the concentration of the desired chlorinated species. Finally, the third method involves the calculation of the thermodynamic equilibrium by minimizing the total Gibbs energy of the system. The concentrations of all species in the phase ensemble are then simultaneously computed.

2.2.1 Methods based on ΔG_r^o x T diagrams

It will be supposed that the oxide M_2O_5 can generate two gaseous chlorinated species, MCl_4 and MCl_5:

$$\begin{aligned} M_2O_5(s) + 5Cl_2(g) &\rightarrow 2MCl_5(g) + \frac{5}{2}O_2(g) \\ M_2O_5(s) + 4Cl_2(g) &\rightarrow 2MCl_4(g) + \frac{5}{2}O_2(g) \end{aligned} \tag{21}$$

The first reaction is associated with a reduction of the number of moles of gaseous species (Δn_g = -0.5), but in the second the same quantity is positive (Δn_g = 0.5). If the gas phase is described as an ideal solution, the first reaction should be associated with a lower molar entropy than the second. The greater the number of mole of gaseous products, the greater the gas phase volume produced, and so the greater the entropy generated. By plotting the molar Gibbs energy of each reaction as a function of temperature, the curves should cross each other at a specific temperature (T_C). For temperatures greater than T_C the formation of MCl_4 becomes thermodynamically more favorable (see Figure 4).

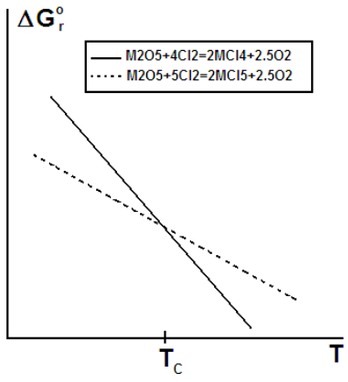

Fig. 4. Hypothetical ΔG_r^o x T curves with intercept.

An interesting situation occurs, if one of the chlorides can be produced in the condensed state (liquid or solid). Let's suppose that the chloride MCl_5 is liquid at lower temperatures.

The ebullition of MCl_5, which occur at a definite temperature (T_t), dislocates the curve to lower values for temperatures higher than T_t. Such an effect would make the production of MCl_5 in the gaseous state thermodynamically more favorable even for temperatures greater than T_c (Figure 5). Such fact the importance of considering phase transitions when comparing ΔG_r^o x T curves for different reactions.

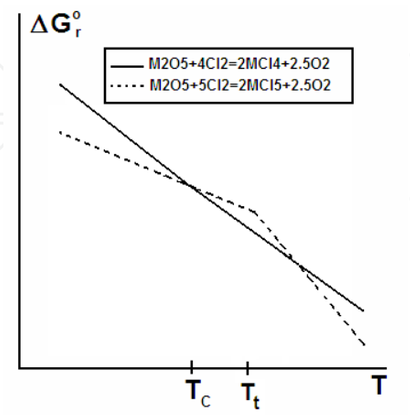

Fig. 5. Effect of MCl_5 boiling temperature

Although simple, the method based on the comparison of ΔG_r^o x T diagrams is of limited application. The problem is that for discussing the thermodynamic viability of a reaction one must actually compute the thermodynamic driving force (Eq. 15 and 16), and by doing so, one must fix values for the concentration of Cl_2 and O_2 in the reactor's atmosphere, which, in the end, define the value of the reaction coefficient.

If the ΔG_r^o x T curves of two reactions lie close to one another (difference lower than 10 KJ/mol), it is impossible to tell, without a rigorous calculation, which chlorinated specie should have the highest concentration in the gaseous state, as the computed driving forces will lie very close from each other. In these situations, other methods that can address the direct effect of the reactor's atmosphere composition should be applied.

Apart from its simplicity, the ΔG_r^o x T diagrams have another interesting application in relation to the proposal of reactions mechanisms. From the point of view of the kinetics, the process of forming higher chlorinated species by the "collision" of one molecule of the oxide M_2O_5 and a group of molecules of Cl_2, and vise versa, shall have a lower probability than the one defined by the first formation of a lower chlorinated specie, say MCl_2, and the further reaction of it with one or two Cl_2 molecules (Eq. 22).

Let's consider that M can form the following chlorides: MCl, MCl_2, MCl_3, MCl_4, and MCl_5. The synthesis of MCl_5 can now be thought as the result of the coupled reactions represented by Eq. (22).

$$\begin{aligned} &M_2O_5 + Cl_2 \rightarrow 2MCl + 2.5O_2 \\ &MCl + 0.5Cl_2 \rightarrow MCl_2 \quad MCl_2 + 0.5Cl_2 \rightarrow MCl_3 \\ &MCl_3 + 0.5Cl_2 \rightarrow MCl_4 \quad MCl_4 + 0.5Cl_2 \rightarrow MCl_5 \end{aligned} \tag{22}$$

By plotting the ΔG_r^o x T diagrams of all reactions presented in Eq. (22) it is possible to evaluate if the thermodynamic stability of the chlorides follows the trend indicated by the

proposed reaction path. If so, the curves should lay one above the other. The standard reaction Gibbs energy would then grow in the following order: MCl, MCl_2, MCl_3, MCl_4 and MCl_5 (Figure 6).

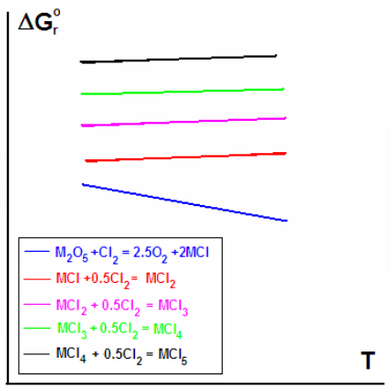

Fig. 6. Hypothetic ΔG_r^o x T curves for successive chlorination reactions

Another possibility is that the curve for the formation of one of the higher chlorinated species is associated with lower Gibbs energy values in comparison with the curve of a lower chlorinated compound. A possible example thereof is depicted on Figure (7), where the ΔG_r^o x T curve for the production of MCl_3 lies bellow the curve associated with the formation of MCl_2.

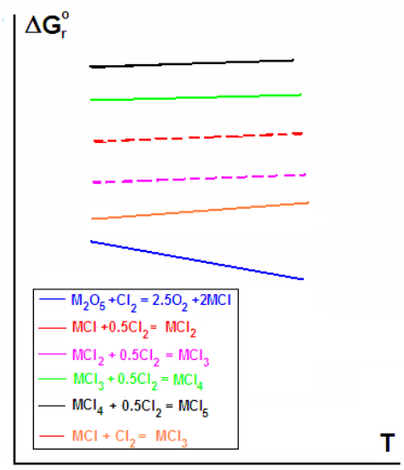

Fig. 7. Successive chlorination reactions – direct formation of MCl_3 from MCl

The formation of the species MCl_2 would be thermodynamically less favorable, and MCl_3 is preferentially produced directly from MCl ($MCl + Cl_2 = MCl_3$). In this case, however, for the diagram to remain thermodynamically consistent, the curves associated with the formation of MCl_2 from MCl and MCl_3 from MCl (broken lines) should be substituted for the curve associated with the direct formation of MCl_3 from MCl for the entire temperature range.
The same effect could originate due to the occurrence of a phase transition. Let's suppose that in the temperature range considered MCl_3 sublimates at T_s. Because of this

phenomenon the curve for the formation of MCl_2 crosses the curve for the formation of the last chloride at T_c, so that for $T > T_c$ its formation is associated with a higher thermodynamic driving force (Figure 8). So, for $T > T_c$, MCl_3 is formed directly from MCl, resulting in the same modification in the reaction mechanism as mentioned above.

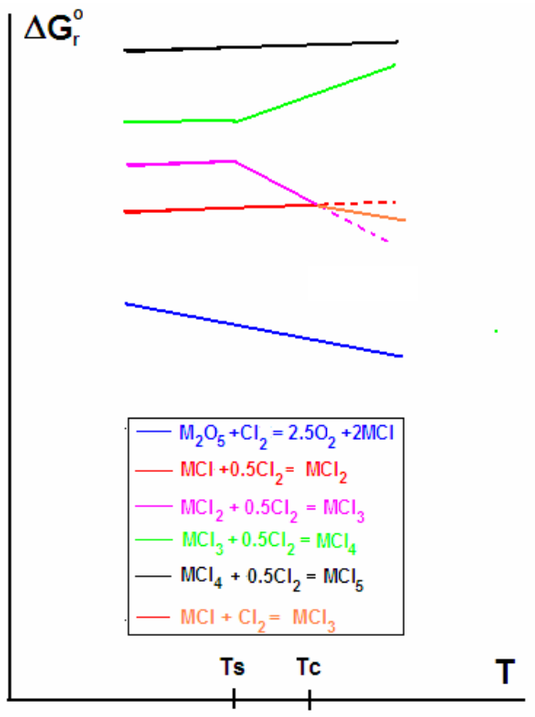

Fig. 8. Direct formation of MCl_3 from MCl stimulated by MCl_3 sublimation

For temperatures higher than T_c, the diagram of Figure (8) looses its thermodynamic consistency, as, according to what was mentioned in the last paragraph, the formation of MCl_2 from MCl is impossible in this temperature range. The error can be corrected if, for $T > Tc$, the curves associated with the formation of MCl_2 and MCl_3 (broken lines) are substituted for the curve associated with the formation of MCl_3 directly from MCl.

A direct consequence of that peculiar thermodynamic fact, as described in Figures (7) and (8), is that under these conditions, a predominance diagram would contain a straight line showing the equilibrium between MCl and MCl_3, and the field corresponding to MCl_2 would not appear.

2.2.2 Method of Kang and Zuo

Kang & Zuo (1989) introduced a simple method for comparing the thermodynamic tendencies of formation of compounds obtained by gas – solid reactions, in that each equilibrium equation is solved independently, and the concentration of the desired species plotted as a function of the gas phase concentration and or temperature. The method will be illustrated for the reactions defined by Eq. (21). The concentrations of MCl_4 and MCl_5 in the gaseous phase can be computed as a function of temperature, partial pressure of Cl_2, and partial pressure of O_2.

$$P_{MCl_5} = \sqrt{\frac{{P_{Cl_2}}^5}{{P_{O_2}}^{5/2}} \exp\left(-\frac{\left(2g^g_{MCl_5} + \frac{5}{2}g^g_{O_2} - 5g^g_{Cl_2} - g^s_{M_2O_5}\right)}{RT}\right)}$$

$$P_{MCl_4} = \sqrt{\frac{{P_{Cl_2}}^4}{{P_{O_2}}^{5/2}} \exp\left(-\frac{\left(2g^g_{MCl4} + \frac{5}{2}g^g_{O2} - 4g^g_{Cl2} - g^s_{M2O5}\right)}{RT}\right)} \quad (23)$$

Next, two intensive properties must be chosen, whose values are fixed, for example, the partial pressure of Cl_2 and the temperature. The partial pressure of each chlorinated species becomes in this case a function of only the partial pressure of O_2.

$$\begin{aligned}
P_{MCl_5} &= f_{MC_5}\left(T, P_{Cl_2}\right) {P_{O_2}}^{5/2} \\
P_{MCl_4} &= f_{MCl_4}\left(T, P_{Cl_2}\right) P_{O_2}^{5/2} \\
f_{MCl_5}\left(T, P_{Cl_2}\right) &= {P_{Cl_2}}^{-5/2} \exp\left(-\frac{\left(2g^g_{MCl_5} + \frac{5}{2}g^g_{O_2} - 5g^g_{Cl_2} - g^s_{M_2O_5}\right)}{2RT}\right) \\
f_{MCl_4}\left(T, P_{Cl_2}\right) &= {P_{Cl_2}}^{-2} \exp\left(-\frac{\left(2g^g_{MCl_4} + \frac{5}{2}g^g_{O_2} - 4g^g_{Cl_2} - g^s_{M_2O_5}\right)}{2RT}\right)
\end{aligned} \quad (24)$$

By fixing T and $P(Cl_2)$ the application of the natural logarithm to both sides of Eq. (24) results in a linear behavior.

$$\begin{aligned}
\ln P_{MCl_5} &= \ln f_{MCl_4} + 2.5 \ln P_{O_2} \\
\ln P_{MCl_4} &= \ln f_{MCl_5} + 2.5 \ln P_{O_2}
\end{aligned} \quad (25)$$

The lines associated with the formation of MCl_4 and MCl_5 would have the same angular coefficient, but different linear coefficients. If the partial pressure of Cl_2 is equal to one (pure Cl_2 is injected into the reactor), the differences in the standard reaction Gibbs energy controls the values of the linear coefficients observed. If the lowest Gibbs energy values are associated with the formation of MCl_5, its line would have the greatest linear coefficient (Figure 9).

An interesting situation occurs if the curves obtained for the chlorinated species of interest cross each other (Figure 10). This fact would indicate that for some critical value of $P(O_2)$ there would be a different preference for the system to generate each one of the chlorides. One of them prevails for higher partial pressure values and the other for values of $P(O_2)$ lower than the critical one. Such a behavior could be exemplified if the chlorination of M also generates the gaseous oxychloride $MOCl_3$ ($M_2O_5 + 2Cl_2 = 2MOCl_3 + 1.5O_2$).

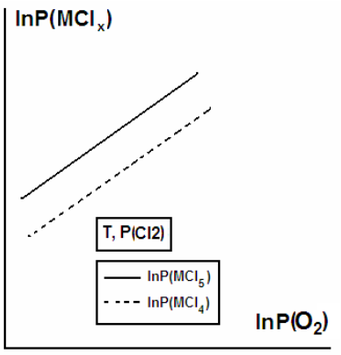

Fig. 9. Concentrations of MCl_4 and MCl_5, as a function of $P(O_2)$

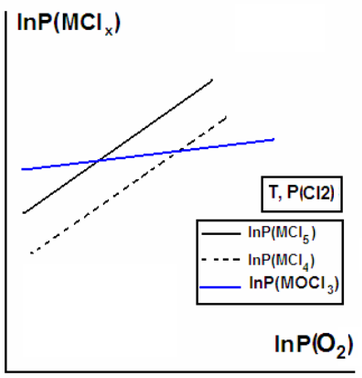

Fig. 10. Concentrations of $MOCl_3$, MCl_4 and MCl_5 as a function of $P(O_2)$

$$\ln P_{MOCl_3} = \ln f_{MOCl_3} + 1.5 \ln P_{O_2} \tag{26}$$

The linear coefficient of the line associated with the $MOCl_3$ formation is higher for the initial value of $P(O_2)$ than the same factor computed for MCl_4 and MCl_5. As the angular coefficient is lower for $MOCl_3$, The graphic of Figure (10) depicts a possible result.

According to Figure (10), three distinct situations can be identified. For the initial values of $P(O_2)$, the partial pressure of $MOCl_3$ is higher than the partial pressure of the other chlorinated compounds.

By varying $P(O_2)$, a critical value is approached after which $P(MCl_5)$ assumes the highest value, being followed by $P(MOCl_3)$ and then $P(MCl_4)$. A second critical value of $P(O_2)$ can be identified in the graphic above. For $P(O_2)$ values higher than this, the atmosphere should be more concentrated in MCl_5 and less concentrated in $MOCl_3$, MCl_4 assuming a concentration value in between.

2.2.3 Minimization of the total gibbs energy

The most general way of describing equilibrium is to fix a number of thermodynamic variables (physical parameters that can be controlled in laboratory), and to chose an appropriate thermodynamic potential, whose maxima or minima describe the possible equilibrium states available to the system.

By fixing T, P, and total amounts of the components M, O, and Cl (n(O), n(M), and n(Cl)), the global minimum of the total Gibbs energy describes the equilibrium state of interest,

which is characterized by a proper phase ensemble, their amounts and compositions. This method is equivalent to solve all chemical equilibrium equations at the same time, so, that the compositions of the chlorinated species in each one of the phases present are calculated simultaneously.

For treating the equilibrium associated with the chlorination processes, two type of diagrams are important: *predominance diagrams*, and *phase speciation diagrams*. The first sort of diagram describes the equilibrium phase ensemble as a function of temperature, and or partial pressure of Cl_2 or O_2. The second type describes how the composition of individual phases varies with temperature and or concentration of Cl_2 or O_2.

The first step is to change the initial constraint vector (T, P, n(O), n(M), n(Cl)), by modifying the definition of the components. Instead considering as components the elements O, M, and Cl, we can describe the global composition of the system by specifying amounts of M, Cl_2 and O_2 (T, P, $n(O_2)$, n(M), $n(Cl_2)$).

According to the phase-rule (Eq. 27) applied to a system with three components (M, Cl_2 and O_2), by specifying five degrees of freedom (intensive variables or restriction equations) the equilibrium calculation problem has a unique solution:

$$\begin{aligned} L &= C + 2 - F \\ F &= 0 \quad C = 3 \\ L &= 5 \end{aligned} \tag{27}$$

Where F denotes the number of phases present (as we do not know the nature of the phase ensemble, $F = 0$ at the beginning), C is the number of components, and L defines the number of degrees of freedom (equations and or intensive variables) to be specified. So, with $L = 5$, the constraint vector must have five coordinates (T, P, $n(O_2)$, n(M), $n(Cl_2)$).

In reality, the chlorination system is described as an open system, where a gas flux of definite composition is established. The constraint vector defined so far is consistent with the definition of a closed system, which by definition does not allow matter to cross its boundaries. The calculation can become closer to the physical reality of the process if we specify the chemical activities of Cl_2 and O_2 in the gas phase, instead of fixing their global molar amounts. Such a restriction would be analogous as fixing the inlet gas composition. Further, if the gas is considered to behave ideally, the chemical activities can be replaced by the respective values of the partial pressure of the gaseous components. So, the final constraint vector should be defined as follows: T, P, n(M), $P(Cl_2)$, $P(O_2)$.

The two types of computation mentioned in the first paragraph can now be discussed. For generating a speciation diagram, only one of the parameters T, $P(Cl_2)$, or $P(O_2)$ is varied in a definite range. The composition of some phase of interest, for example the gas, can then be plotted as a function of the thermodynamic coordinate chosen. On the other hand, by systematically varying two of the parameter defined in the group T, $P(Cl_2)$, or $P(O_2)$, a predominance diagram can be constructed (Figure 11). The diagram is usually drawn in space $P(Cl_2)$ x $P(O_2)$ and is composed by cells, which describe the stability limits of individual phases. A line describes the equilibrium condition involving two phases, and a point the equilibrium involving three phases.

Let's take a closer look in the nature of a predominance diagram applied to the case studied so far. In this situation, one must consider the gas phase, the solid metal M, and possible oxides, MO, MO_2, and M_2O_5, obtained through oxidation of the element M at different oxygen potentials. The equilibrium involving two oxides defines a unique value of the partial pressure of O_2, which is independent of the Cl_2 concentration.

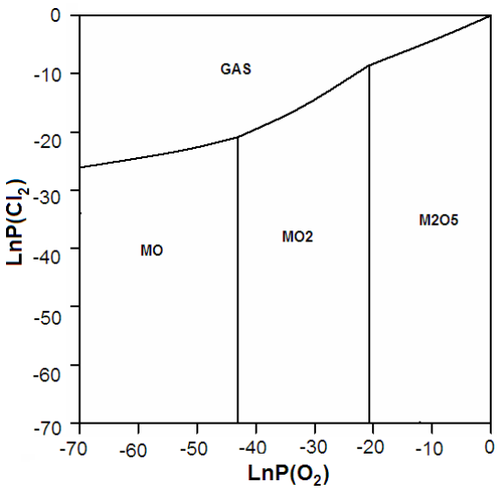

Fig. 11. Hypothetical predominance diagram chlorides mixed in the gas phase

For the equilibrium between MO and MO_2, for example, Eq. (28) enables the determination of the $P(O_2)$ value, which is fixed by choosing T and is independent of the Cl_2 partial pressure. As a consequence, such equilibrium states are defined by a vertical line.

$$P_{O_2} = \exp\left(-\frac{\left(g^{s}_{MO_2} - g^{s}_{MO} - 0.5g^{g}_{O_2}\right)}{RT}\right) \tag{28}$$

The equilibrium when the phase ensemble is defined by the gas and one of the metal oxides, say MO_2, is also defined by a line, whose inclination is determined by fixing T, P, $n(M)$ and $P(O_2)$. This time the concentration of Cl_2, MCl_4 and MCl_5 are computed by solving the group of non-linear equations presented bellow (Eq. 29). The first equation defines the restriction that the molar quantity of M is constant (mass conservative restriction). The second equation represents the conservation of the total mass of the gas phase (the summation of all mol fractions must be equal to one).

$$\begin{aligned}
&n_M = n_{MO_2} + n^{g}\left(x^{g}_{MCl_4} + x^{g}_{MCl_5}\right)\\
&1 = x^{g}_{MCl_4} + x^{g}_{MCl_5} + x^{g}_{O_2} + x^{g}_{Cl_2}\\
&\mu^{g}_{MCl_5} - \mu^{g}_{MCl_4} - \frac{\mu^{g}_{Cl_2}}{2} = 0\\
&2\mu^{g}_{MCl5} + 2.5\mu^{g}_{O_2} - g^{s}_{M_2O_5} - 5\mu^{g}_{Cl_2} = 0\\
&2\mu^{g}_{MCl_4} + 2.5\mu^{g}_{O_2} - g^{s}_{M_2O_5} - 4\mu^{g}_{Cl_2} = 0
\end{aligned} \tag{29}$$

The other three relations define, respectively, the equilibrium conditions for the following group of reactions:

$$\begin{aligned}
&MCl_4(g) + 0.5Cl_2(g) \rightarrow MCl_5(g)\\
&MO_2(s) + 2.5Cl_2(g) \rightarrow MCl_5(g) + O_2(g)\\
&MO_2(s) + 2Cl_2(g) \rightarrow MCl_4(g) + O_2(g)
\end{aligned} \tag{30}$$

So, we have five equations and five unknowns (n^g , n_{MO_2} , $x^g_{MCl_4}$, $x^g_{MCl_5}$, $x^g_{Cl_2}$), indicating that the equilibrium calculation admits a unique solution.

Finally by walking along a vertical line associated with the coexistence of two metallic oxides, for example MO and MO_2, a condition is achieved where the gaseous chlorides are formed. The equilibrium between the two oxides and the gas phase is defined by a point. In other words by fixing *T* and *P*, all equilibrium properties are uniquely defined. The equation associated with the coexistence of MO and MO_2 (Eq. 28) is added and the partial pressure of O_2 is allowed to vary, resulting in six variables and six equations (Eq. 31).

Equations (30) and (31) were presented here only with a didactic purpose. In praxis, the majority of the thermodynamic software (*Thermocalc*, for example) are designed to minimize the total Gibbs energy of the system. The algorithm varies systematically the composition of the equilibrium phase ensemble until the global minimum is achieved. By doing so the same algorithm can be implemented for dealing with all possible equilibrium conditions, eliminating at the end the difficulty of proposing a group of linear independent chemical equations, which for a system with a great number of components can become a complicated task.

$$
\begin{aligned}
& n_M = n_{MO_2} + n^g \left(x^g_{MCl_4} + x^g_{MCl_5} \right) \\
& 1 = x^g_{MCl_4} + x^g_{MCl_5} + x^g_{O_2} + x^g_{Cl_2} \\
& \mu^g_{MCl_5} - \mu^g_{MCl_4} - 0.5\mu^g_{Cl_2} = 0 \\
& 2\mu^g_{MCl_5} + 2.5\mu^g_{O_2} - g^s_{M_2O_5} - 5\mu^g_{Cl_2} = 0 \\
& 2\mu^g_{MCl_4} + 2.5\mu^g_{O_2} - g^s_{M_2O_5} - 4\mu^g_{Cl_2} = 0 \\
& g^s_{MO_2} - g^s_{MO} - 0.5\mu^g_{O_2} = 0
\end{aligned}
\tag{31}
$$

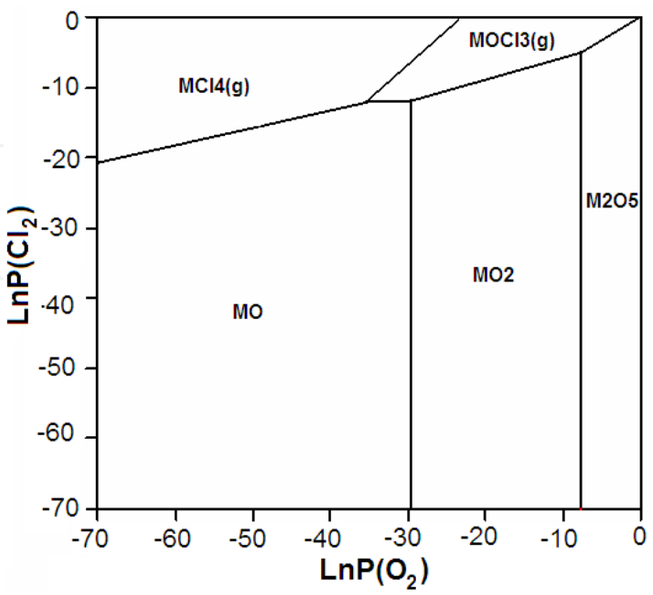

Fig. 12. Hypothetical predominance diagram: pure gaseous chlorides

A simplified version of the predominance diagram of Figure (11) can be achieved through considering each possible gaseous chloride as a pure substance. In this case, the field representing the gas phase will be divided into sub-regions, each one representative of the stability of each gaseous chlorinated compound. By considering, that, besides MCl_5 and MCl_4, gaseous $MOCl_3$ can also be formed, a diagram similar to the one presented on Figure (12) would represent possible stability limits found in equilibrium.

The diagram of Figure (12) is associated with a temperature value where gaseous MCl_5 can not be present in equilibrium for any suitable value of $P(Cl_2)$ and $P(O_2)$ chosen. It is interesting to note, that in this sort of diagram, there is a direct relation between the inclination of a line representative of the equilibrium between a gaseous chloride or oxychloride and an oxide, with the stoichiometric coefficients of the chemical reaction behind the transformation.

According to Eq. (32), the inclination of the line associated with the equilibrium between $MOCl_3$ and MO_2 should be lower than the one associated with the equilibrium between $MOCl_3$ and M_2O_5. On the other hand, in the case of the equilibrium between MO and $MOCl_3$, the line is horizontal (does not depend on $P(O_2)$), as the same number of oxygen atoms is present in the reactant and products, so O_2 does not participate in the reaction.

$$\begin{aligned} \ln P_{Cl_2} &= \frac{1}{3}\ln P_{O_2} - \frac{2}{3}\ln K_{MO_2}(T) \\ \ln P_{Cl_2} &= \frac{1}{2}\ln P_{O_2} - \frac{1}{3}\ln K_{M_2O_5}(T) \\ \ln P_{Cl_2} &= -\frac{2}{3}\ln K_{MO}(T) \end{aligned} \tag{32}$$

Where, K_{MO_2} , $K_{M_2O_5}$ and K_{MO} represent respectively the equilibrium constants for the formation of $MOCl_3$ from MO_2, M_2O_5 and MO (Eq. 33).

$$\begin{aligned} MO_2 + 1.5Cl_2 &\rightarrow MOCl_3 + 0.5O_2 \\ M_2O_5 + 3Cl_2 &\rightarrow 2MOCl_3 + 1.5O_2 \\ MO + 1.5Cl_2 &\rightarrow MOCl_3 \end{aligned} \tag{33}$$

The diagrams of Figures (11) and (12) depict a behavior, where no condensed chlorinated phases are present. For many oxides, however, there is a tendency of formation of solid or liquid chlorides and or oxychlorides, which must appear in the predominance diagram as fields between the pure oxides and the gas phase regions. Such a behavior can be observed in the equilibrium states accessible to the system V – O – Cl.

3. The system V – O – Cl

Vanadium is a transition metal that can form a variety of oxides. At ambient temperature and oxygen potential, the form V_2O_5 is the most stable. It is a solid stoichiometric oxide, where vanadium occupies the +5 oxidation state. By lowering the partial pressure of O_2, the valence of vanadium varies considerably, making it is possible to produce a family of stoichiometric oxides: V_2O_4, V_3O_5, V_4O_7, VO, VO_2 and V_2O_3. Recently, it has been discovered that vanadium can also form a variety of non-stoichiometric oxygenated compounds (Brewer & Ebinghaus, 1988), however, to simplify the treatment of the present chapter, these

phases will not be included in the data-base used for the following computations. Additionally, it was considered that the concentration of the oxides in gas phase is low enough to be neglected. Further, on what touches the computations that follows, the software *Thermocalc* was used in all cases, and it will always be assumed that equilibrium is achieved, or in other words, kinetic effects can be neglected.
The relative stability of the possible vanadium oxides can be assessed through construction of a predominance diagram in the space T – $P(O_2)$ (see Figure 13). As thermodynamic constraints we have n(V) (number of moles of vanadium metal – it will be supposed that n(V) =1), T, P and $P(O_2)$. The reaction temperature will be varied in the range between 1073 K and 1500 K and the partial pressure of O_2 in the range between $8.2.10^{-40}$atm and 1atm.

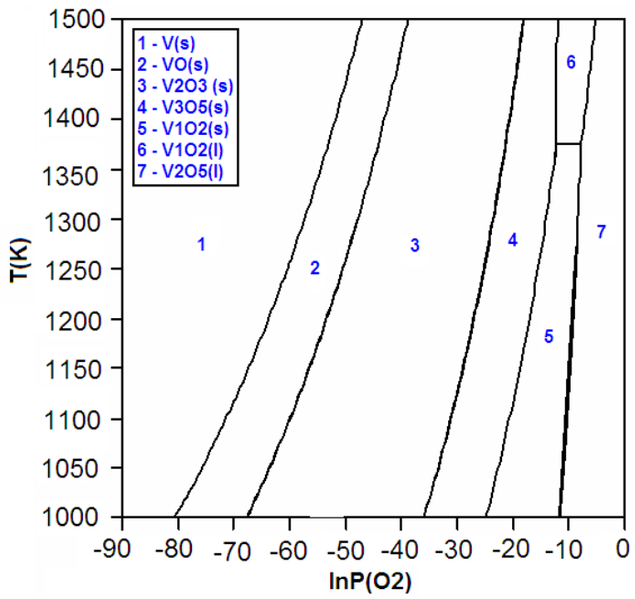

Fig. 13. Predominance diagram for the system V – O

The total pressure was fixed at 1atm. It can be seen that for the temperature range considered and a partial pressure of O_2 in the neighborhood of 1atm, V_2O_5 is formed in the liquid state. Through lowering the oxygen potential, crystalline vanadium oxides precipitate, VO_2 being formed first, followed by V_2O_3, VO, and finally V. The horizontal line between fields "5" and "6" indicates the melting of V_1O_2, which according to classical thermodynamics must occur at a fixed temperature. Next it will be considered the species formed by vanadium, chlorine and oxygen.

3.1 Vanadium oxides and chlorides

The already identified species formed between vanadium, chlorine and oxygen are: VCl, VCl_2, VCl_3, VCl_4, VOCl, $VOCl_2$, $VOCl_3$, VO_2Cl.
On Table (2) it was included information regarding the physical states at ambient conditions and some references related to phase equilibrium studies conducted on samples of specific vanadium chlorinated compounds.
Only a few studies were published in literature in relation to the thermodynamics of vanadium chlorinated phases. On Table (2) some references are given for earlier

investigations associated with measurements of the vapor pressure for the sublimation of VCl_2 and VCl_3, and the boiling of $VOCl_3$ and VCl_4. There are also evidences for the occurrence of specific thermal decomposition reactions (Eq. 34), such as those of VCl_3, $VOCl_2$ and VO_2Cl (Oppermann, 1967).

Chloride	Physical state	Equilibrium data	Reference
VCl	-	-	-
VCl_2	Solid	Sublimation(	McCarley & Roddy (1964)
VCl_3	Solid	Sublimation/ Thermal decomposition	McCarley & Roddy (1964)
VCl_4	Liquid	Ebulition	Oppermann (1962a)
$VOCl_3$	Liquid	Ebulition(	Oppermann (1967)
VO_2Cl	Solid	Thermal decomposition(	Oppermann (1967)
$VOCl_2$	Solid	Thermal decomposition(	Oppermann (1967)
VOCl	Solid	Synthesis and characterization(	Schäffer at al. (1961)

Table 2. Physical nature and phase equilibrium data for vanadium chlorinated compounds

$$\begin{aligned} 2VCl_3(s) &\rightarrow VCl_2(s) + VCl_4(g) \\ 3VO_2Cl(s) &\rightarrow VOCl_3(g) + V_2O_5(s) \\ 2VOCl_2(s) &\rightarrow VOCl_3(g) + VOCl(s) \end{aligned} \tag{34}$$

Chromatographic measurements conducted recently confirmed the possible formation of VCl, VCl_2, VCl_3, and VCl_4 in the gas phase (Hildenbrand et al., 1988). In this study the molar Gibbs energy models for the mentioned chlorides were revised, and new functions proposed. In the case vanadium oxychlorides, models for the molar Gibbs energies of gaseous VOCl, $VOCl_3$, and $VOCl_2$ have already been published (Hackert et al., 1996).
For gaseous VO_2Cl, on the other hand, no thermodynamic model exists, indicating the low tendency of this oxychloride to be stabilized in the gaseous state.

3.1.1 The V – O_2 – Cl_2 stability diagram

The relative stability of the possible chlorinated compounds of vanadium can be assessed through construction of predominance diagrams by fixing the temperature and systematic varying the values of $P(Cl_2)$ and $P(O_2)$.
For the temperature range usually found in chlorination praxis, three temperatures were considered, 1073 K, 1273 K and 1573 K. The partial pressure of Cl_2 and O_2 were varied in the range between $3.98.10^{-31}$atm and 1atm. All chlorinated species are considered to be formed at the standard state (pure at 1atm). The predominance diagrams can be observed on Figures (14), (15) and (16).
The stability field of VCl_2(l) grows in relation to those associated to VCl_4 and $VOCl_3$. At 1573 K the VCl_2(l) area is the greatest among the chlorides and the VCl_3(g) field appears. So, as temperature achieves higher values the concentration of VCl_3 in the gas phase should increase in comparison with the other chlorinated species, including VCl_2. This behavior agrees with the one observed during the computation of the gas phase speciation and will be better discussed on topic (3.1.3.2).

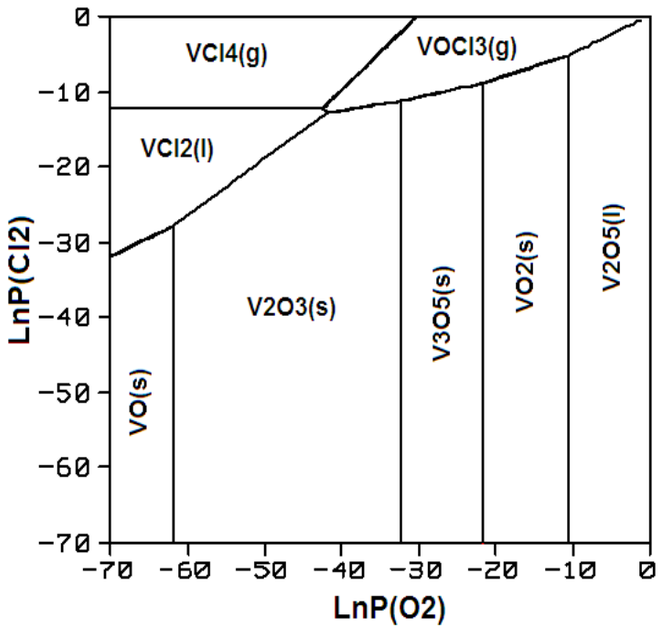

Fig. 14. Predominance diagram for the system V – O – Cl at 1073 K

Finally, by starting in a state inside a field representing the formation of VCl_4 or VCl_3 and by making $P(O_2)$ progressively higher, a value is reached, after which $VOCl_3$(g) appears. So, the mol fraction of VCl_4 and VCl_3 in gas should reduce when $P(O_2)$ achieves higher values. This is again consistent with the speciation computations developed on topic (3.1.3.2).

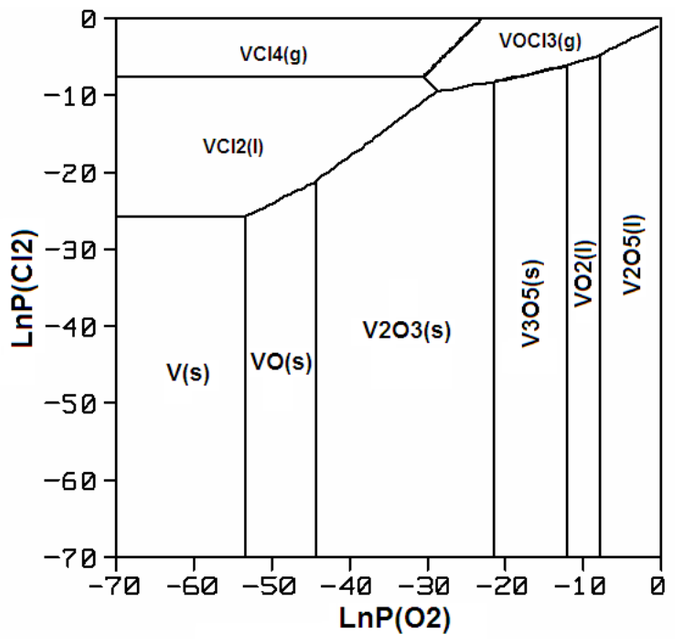

Fig. 15. Predominance diagram for the system V – O – Cl at 1273 K

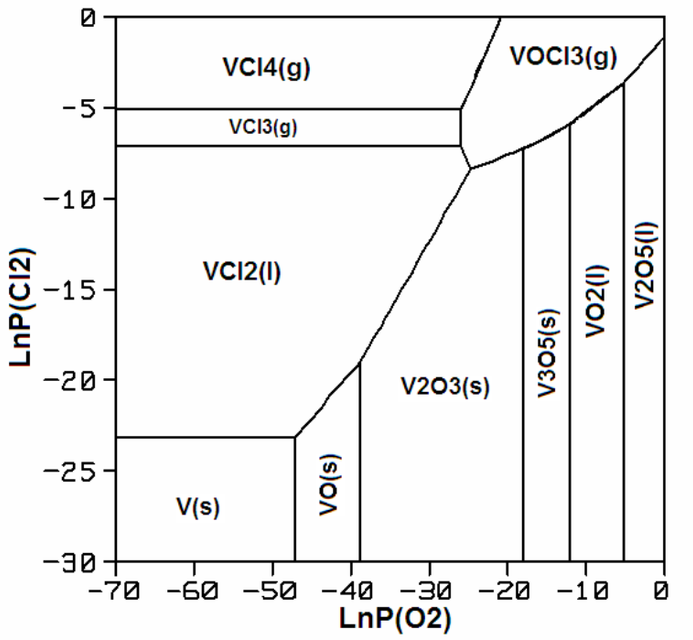

Fig. 16. Predominance diagram for the system V – O – Cl at at 1573 K

3.1.2 V_2O_5 direct chlorination and the effect of the reducing agent

The direct chlorination of V_2O_5 is a process, which consists in the reaction of a V_2O_5 sample with gaseous Cl_2.

$$V_2O_5 + Cl_2 = \text{Chloride/Oxychloride} + O_2 \quad (35)$$

In praxis, temperature lies usually between 1173 K and 1473 K. The chlorination equilibrium could then be dislocated in the direction of the formation of chlorides and oxychlorides if one removes O_2 and or adds Cl_2 to the reactors atmosphere. So, for low $P(O_2)$ (< 10^{-20} atm) and high $P(Cl_2)$ (between 0.1 and 1 atm) values, according to the predominance diagrams of Figures (14) and (15), VCl_4 should be the most stable vanadium chloride, which is produced according to Eq. (36).

$$V_2O_5 + 2Cl_2 = 2VCl_4 + 2.5O_2 \quad (36)$$

K	T (K)
$1.76257.10^{-13}$	1173
$5.82991.10^{-11}$	1273
$1.0397.10^{-08}$	1473

Table 3. Equilibrium constant for the reaction represented by Eq. (37)

The equilibrium constant for reaction represented by Eq. (36) is associated with very low values between 1173 K and 1473 K (see Table 3). So, it can be concluded that the formation of VCl_4 has a very low thermodynamic driving force in the temperature range considered. One possibility to overcome this problem is to add to the reaction system some carbon bearing compound (Allain et al., 1997, Gonzallez et al., 2002a; González et al., 2002b; Jena et

al., 2005). The compound decomposes producing graphite, which reacts with oxygen dislocating the chlorination equilibrium in the desired direction. A simpler route, however, would be to admit carbon as graphite together with the oxide sample into the reactor. If graphite is present in excess, the O_2 concentration in the reactor's atmosphere is maintained at very low values, which are achievable through the formation of carbon oxides (Eq. 37)

$$\begin{aligned} 2C + O_2 &= 2CO \\ C + O_2 &= CO_2 \end{aligned} \tag{37}$$

So, for the production of VCl_4 in the presence of graphite, the reaction of C with O_2 can lead to the evolution of gaseous CO or CO_2 (Eq. 38).

$$\begin{aligned} V_2O_5(s,l) + 4Cl_2(g) + 2.5C(s) &\rightarrow 2VCl_4(l,g) + 2.5CO_2(g) \\ V_2O_5(s,l) + 4Cl_2(g) + 5C(s) &\rightarrow 2VCl_4(l,g) + 5CO(g) \end{aligned} \tag{39}$$

The effect of the presence of graphite over the ΔG_r^o x T curves for the formation of VCl_4 can be seen in the diagram of Figure (17). As a matter of comparison, the plot for the formation of the same species in the absence of graphite is also shown, together with the curves for the reactions associated with the formation of CO and CO_2 for one mole of O_2 (Eq. 37).

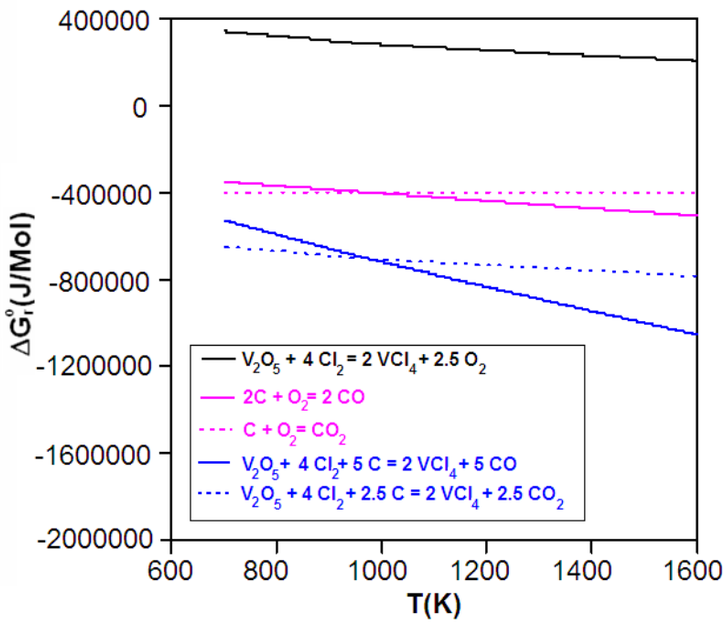

Fig. 17. ΔG_r^o vs. T for for the formation of VCl_4

It can be readily seen that graphite strongly reduces the standard molar Gibbs energy of reaction, promoting in this way considerably the thermodynamic driving force associated with the chlorination process. The presence of graphite has also an impact over the standard molar reaction enthalpy. The direct action of Cl_2 is associated with an endothermic reaction (positive linear coefficient), but by adding graphite the processes become considerably exothermic (negative linear coefficient).

The curves associated with the VCl_4 formation in the presence of the reducing agent cross each other at 973 K, the same temperature where the curves corresponding to the formation of CO and CO_2 have the same Gibbs energy value. This point is defined by the temperature, where the Gibbs energy of the Boudouard reaction ($C + CO_2 = 2CO$) is equal to zero.
The equivalence of this point and the intersection associated with the curves for the formation of VCl_4 can be perfectly understood, as the Boudouard reaction can be obtained through a simple linear combination, according to Eq. (39). So, the molar Gibbs energy associated with the Boudouard reaction is equal to the difference between the molar Gibbs energy of the VCl_4 formation with the evolution of CO and the same quantity for the reaction associated with the CO_2 production. When the curves for the formation of VCl_4 crosses each other, the difference between their molar Gibbs energies is zero, and according to Eq. (39) the same must happen with the molar Gibbs energy of the Boudouard reaction.

$$\begin{aligned}
&1)\ V_2O_5(s,l) + 4Cl_2(g) + 5C(s) \xrightarrow{\Delta G_1} 2VCl_4(l,g) + 5CO(g)\\
&-\\
&2)\ V_2O_5(s,l) + 4Cl_2(g) + 2.5C(s) \xrightarrow{\Delta G_2} 2VCl_4(l,g) + 2.5CO_2(g)\\
&=\\
&3)\ C(s) + CO_2(g) \xrightarrow{\Delta G_3} 2CO(g)
\end{aligned} \tag{39}$$

$$\Delta G_3 = \Delta G_1 - \Delta G_2$$
$$\underset{T\to 973K}{Lim}(\Delta G_3) = \underset{T\to 973K}{Lim}(\Delta G_1 - \Delta G_2) = \Delta G - \Delta G = 0$$

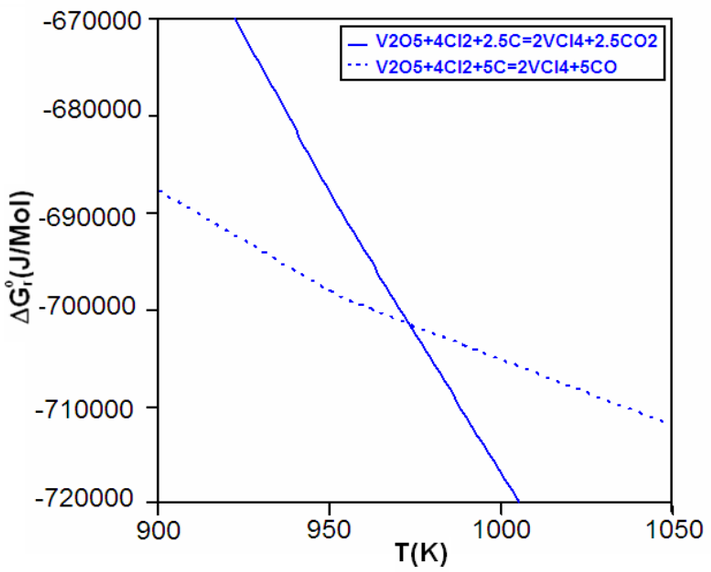

Fig. 18. ΔG_r^o vs. T the formation of VCl_4 – melting of V_2O_5

The inflexion point present on the curves of Figure (17) is associated with the melting of V_2O_5. This inflexion is better evidenced on the graphic of Figure (18). As V_2O_5 is a reactant, according to the concepts developed on topic (2.2.1), the curve should experience a

reduction of its inclination at the melting temperature of the oxide. However, the presence of the inflexion point is much more evident for the reactions with the lowest variation of number of moles of gaseous reactants, as is the case for the direct action of Cl_2, which leads to the evolution of CO_2 ($\Delta n_g = 0.5$).

The quantity Δn_g controls the molar entropy of the reaction. By lowering the magnitude Δn_g the value of the reaction entropy reduces, and the effect of melting of V_2O_5 over the standard molar reaction Gibbs energy becomes more evident.

Based on the predominance diagrams of topic (3.1.1), $VOCl_3$ should be formed for $P(Cl_2)$ close to 1atm as $P(O_2)$ gets higher. The presence of graphite has the same effect over the molar Gibbs energy of formation of $VOCl_3$, promoting in this way the thermodynamic driving force for the reaction. Its curve is compared with the one for the formation of VCl_4 on Figure (19). The inflexion around 954 K is again associated with the melting of V_2O_5. As the reaction associated with the formation of VCl_4, the formation of $VOCl_3$ has a negative molar reaction enthalpy. So, if the gas phase is considered ideal, for the production of both chlorinated compounds the system should transfer heat to its neighborhood (exothermic reaction).

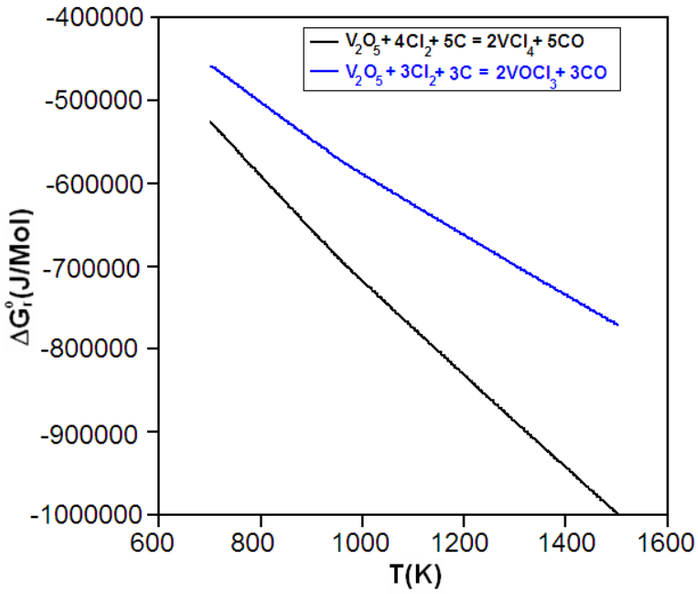

Fig. 19. ΔG_r^o vs. T for the formation of $VOCl_3$ and VCl_4

On what touches the molar reaction entropy, the graphic of Figure (19) indicates, that the reaction associated with the formation of VCl_4 should generate more entropy (more negative angular coefficient for the entire temperature range). This can be explained by the fact, that in the case of VCl_4 the variation of the number of mole of gaseous reactants and products ($\Delta n_g = 3$) is higher than the value for the formation of $VOCl_3$ ($\Delta n_g = 2$). This illustrates how important the magnitude of Δn_g is for the molar entropy of a gas – solid reaction.

Finally, it should be pointed out that the standard molar Gibbs energy has the same order of magnitude for both chlorinated species considered. So, only by appreciating the ΔG_r^o x T curves of these chlorides it is impossible to tell case which species should be found in the gas with the highest concentration. This problem will be covered on topic (3.2).

3.1.2.1 Successive chlorination steps

As discussed on topic (2.2.1), the standard free energy vs. temperature diagram is a valuable tool for suggesting possible reactions paths. Let's consider first the formation of VCl_4. Such a process could be thought as the result of three stages. In the first one, a lower chlorinated compound (VCl) is formed. The precursor then reacts with Cl_2 resulting in higher chlorinated species (Eq. 40).

$$\begin{aligned} &V_2O_5 + Cl_2 + C \rightarrow VCl + CO_2 / CO \\ &VCl + 0.5Cl_2 \rightarrow VCl_2 \\ &VCl_2 + 0.5Cl_2 \rightarrow VCl_3 \\ &VCl_3 + 0.5Cl_2 \rightarrow VCl_4 \end{aligned} \tag{40}$$

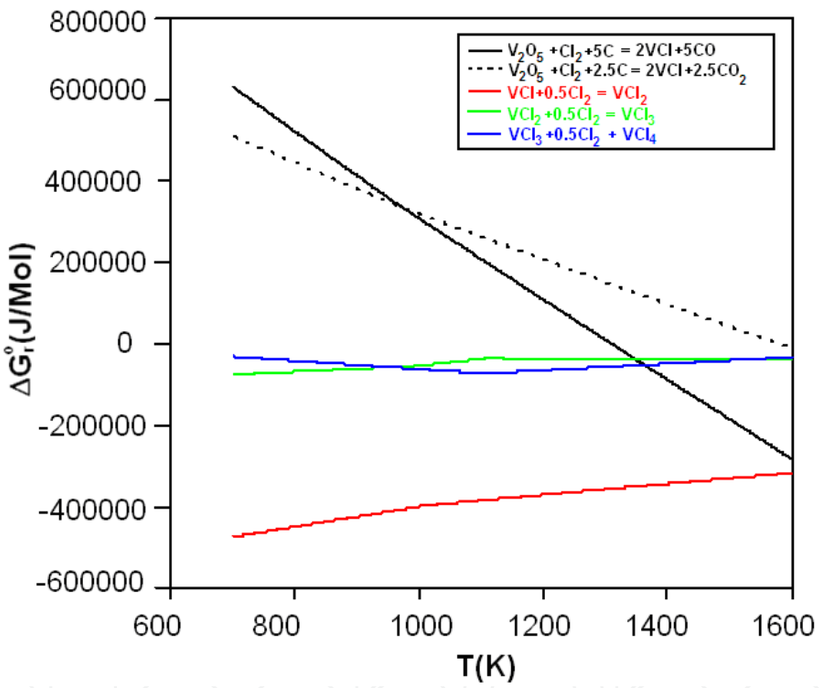

Fig. 20. ΔG_r^o x T for reaction paths of Eq. (38)

The ΔG_r^o x T plots associated with reactions paths represented by mechanisms of Eq. (40) were included on Figure (20). Two inflexion points are evidenced in the diagram of Figure (20). The first one around 1000 K is associated with VCl_2 melting. The second one, around 1100 K, is associated with the sublimation of VCl_3. It can be deduced that only for temperatures greater than 1600 K the path described by Eq. (40) would be possible. For lower temperatures, the molar Gibbs energy of the first step is higher than the one associated with the second.

Another mechanism can be thought for the production of VCl_4. This time, VCl_2 is formed first, which then reacts to give VCl_3 and finally VCl_4 (Eq. 41). The characteristic ΔG_r^o x T curves for the reactions defined in Eq. (41) are presented on Figures (21) and (22).

$$\begin{aligned} V_2O_5 + Cl_2 + C &\rightarrow VCl_2 + CO_2 / CO \\ VCl_2 + 0.5Cl_2 &\rightarrow VCl_3 \\ VCl_3 + 0.5Cl_2 &\rightarrow VCl_4 \end{aligned} \quad (41)$$

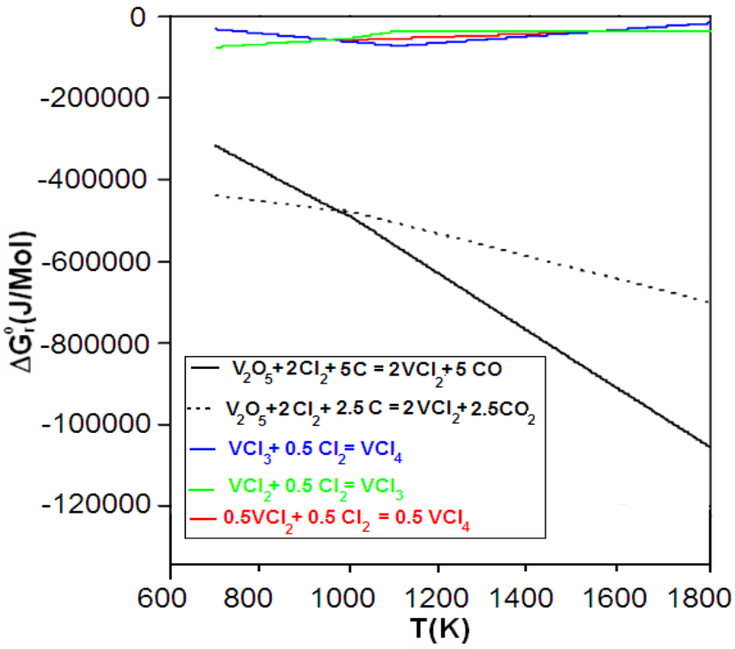

Fig. 21. ΔG_r^o x T for reaction paths of Eq. (41)

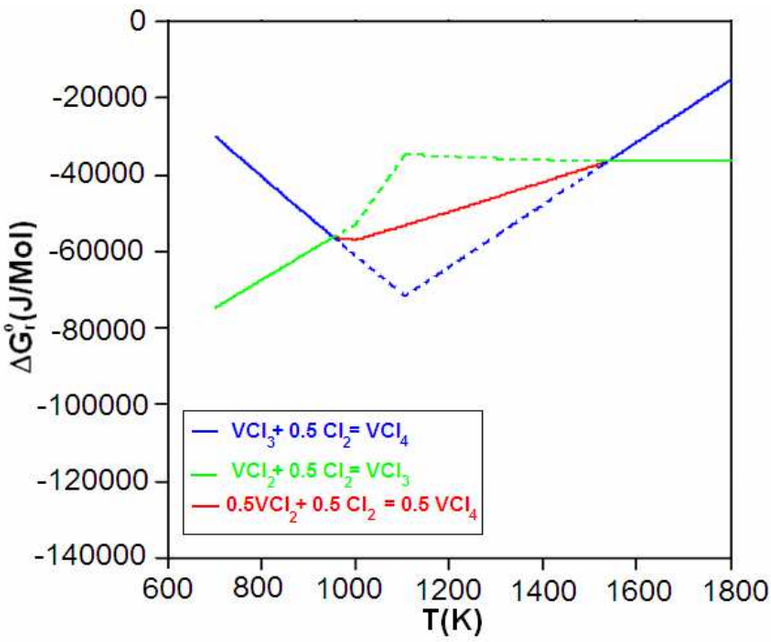

Fig. 22. ΔG_r^o x T for reaction paths of Eq. (41)

The inflexion points have the same meaning as described for diagram of Figure (20). It can be seen that the first step has a much higher thermodynamic tendency as the other. Also, for temperatures lower than 953 K the second step leads to the formation of VCl_3, which then reacts to give VCl_4. However, for temperatures higher than 953 K and lower than 1539 K, the step associated with the formation of VCl_4 is the one with the lowest standard Gibbs energy. So, in this temperature range, VCl_4 should be formed directly from VCl_2, as suggested by Eq. (42). In order to achieve thermodynamic consistency in the mentioned temperature interval, the curves associated with the formation of VCl_3 and VCl_4 according to Eq. (41) should be substituted for the curve associated with reaction defined by Eq. (42), which was represented with red color in the plots presented on Figures (21) and (22).

$$VCl_2 + Cl_2 = VCl_4 \tag{42}$$

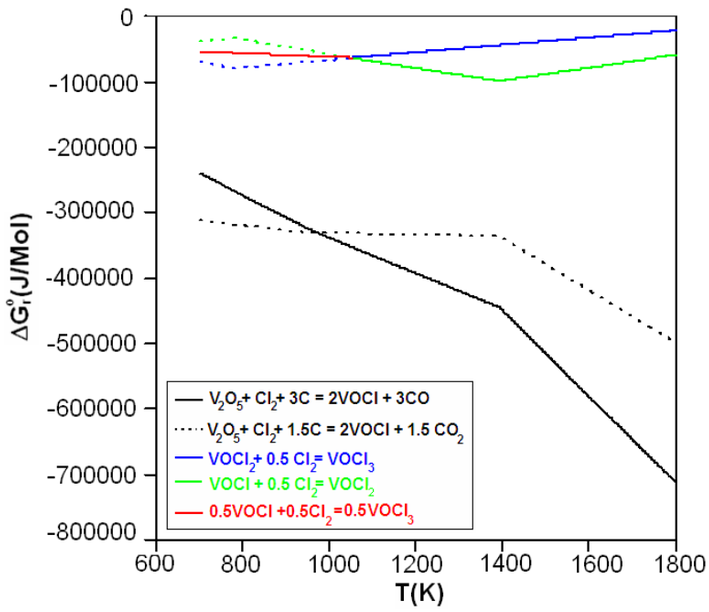

Fig. 23. ΔG_r^o x T for reaction paths of Eq. (43)

For temperatures higher than 1539 K, however, the mechanism is again described by Eq. (41), VCl_3 being formed first, which then reacts leading to VCl_4. It is also interesting to recognize that the sublimation of VCl_3 is responsible for the inversion of the behavior for temperatures higher than approximately 1400 K, where the second reaction step is again the one with the second lowest Gibbs energy of reaction.

On what touches the synthesis of $VOCl_3$, a reaction path can be proposed (Eq. 43), in that VOCl is formed first, which then reacts to give $VOCl_2$, which by itself then reacts to form $VOCl_3$. The ΔG_r^o x T diagrams associated with these reactions are presented on Figure (23).

$$\begin{gathered} V_2O_5 + Cl_2 + C \rightarrow VOCl + CO/CO_2 \\ VOCl + 0.5Cl_2 \rightarrow VOCl_2 \\ VOCl_2 + 0.5Cl_2 \rightarrow VOCl_3 \end{gathered} \tag{43}$$

The inflexion point around 800 K is associated with the sublimation of $VOCl_2$, and around 1400 K with the sublimation of VOCl. According to the ΔG_r^o x T curves presented on Figure (23), it can be deduced that the reaction steps will follow the proposed order only for temperatures higher than 1053 K. At lower temperatures $VOCl_2$ should be formed directly from VOCl (Eq. 44). It is interesting to note that the sublimation of $VOCl_2$ is the phenomenon responsible for the described inversion of behavior. Again, to attain thermodynamic consistency for temperatures higher than 1053 K, the curves associated with the formation of $VOCl_2$ and $VOCl_3$ according to Eq. (43) must be substituted for the curve associated with reaction represented by Eq. (44), which was drawn with red color in the diagram plotted on Figure (23). It should be mentioned indeed, that the reaction equations compared must be written with the same stoichiometric coefficient for Cl_2, or equivalently, the Gibbs energy of reaction (44) must be multiplied by 1/2.

$$VOCl + Cl_2 = VOCl_3 \tag{44}$$

Finally, some remarks may be constructed about the possible reaction order values in relation to Cl_2. According to the discussion developed so far, for the temperature range between 1100 K and 1400 K, Eq. (45) describes the most probable reactions paths for the formation of VCl_4 and $VOCl_3$. As a result, depending on the nature of the slowest step, the reaction order in respect with Cl_2 can be equal to one, two or ½.

$$\begin{aligned} &V_2O_5 + 2Cl_2 + 5C \rightarrow 2VCl_2 + 5CO \\ &VCl_2 + Cl_2 \rightarrow VCl_4 \\ &V_2O_5 + Cl_2 + 5C \rightarrow 2VOCl + 5CO \\ &VOCl + 0.5Cl_2 \rightarrow VOCl_2 \\ &VOCl_2 + 0.5Cl_2 \rightarrow VOCl_3 \end{aligned} \tag{45}$$

3.1.3 Relative stability of VCl_4 and $VOCl_3$

As is evident from the discussion developed on topic (3.1.2), the chlorinated compounds VCl_4 and $VOCl_3$ are the most stable species in the gas phase as the atmosphere becomes concentrated in Cl_2. The relative stability of these two chlorinated compounds will be first accessed on topic (3.1.3.1) by applying the method introduced by Kang & Zuo (1989) and secondly on topic (3.1.3.2) through computing some speciation diagrams for the gas phase.

3.1.3.1 Method of Kang and Zuo

As shown in thon topic (2.2.2) the concentrations of VCl_4 and $VOCl_3$ can be directly computed by considering that each chlorinated compound is generated independently. It will be assumed that the inlet gas is composed of pure Cl_2 ($P(Cl_2)$ = 1 atm). Further, two temperature values were investigated, 1073 K and 1373 K. At these temperatures, the presence of graphite makes the atmosphere richer in CO, so that for the computations the following reactions will be considered:

$$\begin{aligned} &V_2O_5 + 4Cl_2 + 5C \rightarrow 2VCl_4 + 5CO \\ &V_2O_5 + 3Cl_2 + 5C \rightarrow 2VOCl_3 + 3CO \end{aligned} \tag{46}$$

The concentrations of $VOCl_3$ and VCl_4 can then be expressed as a function of P(CO) and temperature according to Eq. (47).

$$P_{VCl_4} = \sqrt{P_{CO}^5 K_1} \rightarrow \ln P_{VCl_4} = \frac{\ln K_1}{2} + \frac{5}{2}\ln P_{CO}$$
$$P_{VOCl_3} = \sqrt{P_{CO}^3 K_2} \rightarrow \ln P_{VOCl_3} = \frac{\ln K_2}{2} + \frac{3}{2}\ln P_{CO} \quad (47)$$

Where K_1 and K_2 represent, respectively, the equilibrium constants for the reactions associated with the formation of VCl_4 and $VOCl_3$ (Eq. 46). By applying Eq. (47) the partial pressure of VCl_4 and $VOCl_3$ were computed as a function of P(CO). The results were plotted on graphic contained in Figure (24). The significant magnitude of the partial pressure values computed for $VOCl_3$ and VCl_4 is a consequence of the huge negative standard Gibbs energy of reaction associated with the formation of these species in the temperature range considered (see Figure 19).

According to Figure (24), VCl_4 is the chloride with the highest partial pressure for both specified temperatures. Also, for both temperatures, $P(VOCl_3)$ becomes higher than $P(VCl_4)$ only for significant values of P(CO). At 1073 K, for example, the partial pressures of the species have equal values only for P(CO) equal to $2.98.10^3$atm, and at 1373 K the same happens for P(CO) equal to $8.91.10^3$atm.

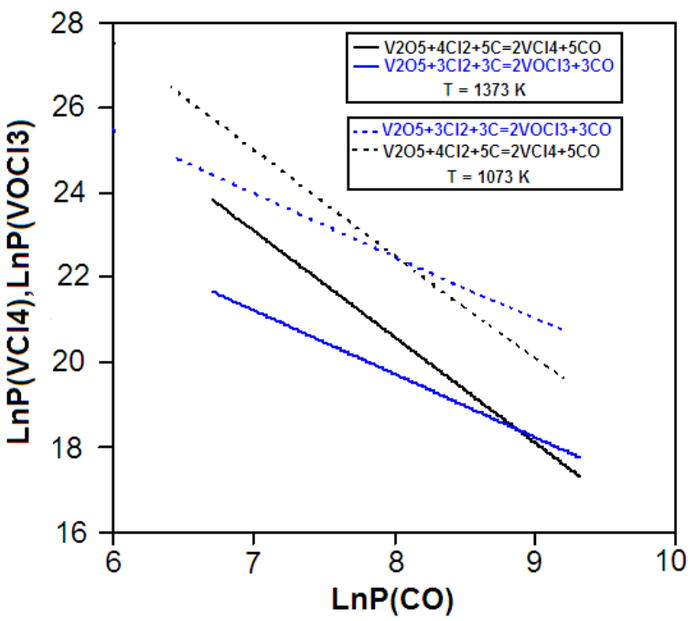

Fig. 24. Ln(P(VCl4)) and Ln(P(VOCl3)) as a function of Ln(P(CO))

As a result, it is expected that the formation of gaseous VCl_4 should have a much greater tendency of occurrence in the temperature range studied. These results will be confirmed through construction of speciation diagrams for the gas phase, a task that will be accomplished on topic (3.1.3.2).

3.1.3.2 Gas phase speciation

The construction of speciation diagrams for the gas phase enables the elaboration of a complementary picture of the chlorination process in question. The word "speciation" means the concentration of all species in gas. This brings another level of complexity to the

quantitative description of equilibrium, as the species build a solution, and as so, their concentrations must be determined at the same time. This sort of information can only arises if one solves the system o equilibrium equations associated to all possible chemical reactions involving the species that form the gas. For the present system (V – O – Cl – C) this task becomes very tricky, as the number of possible species present is pretty significant (ex. CO, CO_2, O_2, VCl_2, VCl_3, VCl, VCl_4, $VOCl_3$, VOCl), and so the number of possible chemical reactions connecting them. So, we must think in another route for simultaneously computing the concentration of the gaseous species produced by our chlorination process. The only possible way consists in minimizing the total Gibbs energy of the system (see topic 2.2.3).

The equilibrium state is defined by fixing T, P, $n(V_2O_5)$, $P(O_2)$ and $P(Cl_2)$. The number of moles of V_2O_5 is fixed at one. If graphite is present in excess, the partial pressure of O_2 is controlled by according to the Boudouard equilibrium (Eq. 39), so that, its presence forces $P(O_2)$ to attain very low values (typically lower than 10^{-20}atm). The total pressure is fixed at 1atm and T varies in the range between 1073 K and 1473 K.

An excess of graphite is desirable, so that the chlorination reactions can achieve a considerable driving force at the desired conditions. Computationally speaking, this can be done in two ways. One possibility is to define an amount of carbon much greater than the number of moles of V_2O_5. Other possibility, which has been made accessible through modern computational thermodynamic software, consists in defining the phase "solid graphite" as fixed with a definite amount. The equilibrium compositions (intensive variables) are not a function of the amount of phases present (size of the system), depending only of temperature and total pressure. So we are free to choose any suitable value we desire, such for example zero ($n_{graphite}$ = 0). This last alternative was implemented in the computations conducted in the present topic.

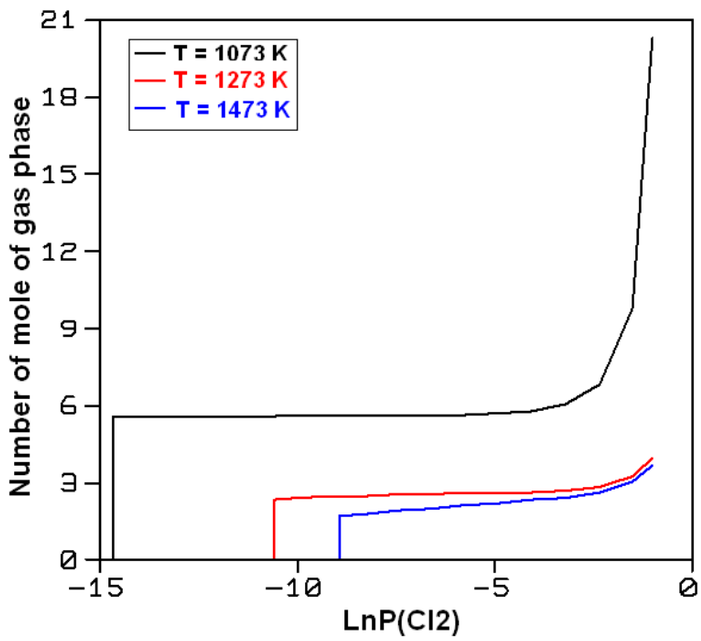

Fig. 25. Number of moles of gas as a function of $P(Cl_2)$

On Figure (25), the number of moles of gas produced was plotted as a function of $P(Cl_2)$ for T equal to 1073 K, 1273 K, and 1473 K. The partial pressure of O_2 was fixed at $1.93.10^{-22}$ atm, and the partial pressure of Cl_2 is varied between $3.6.10^{-7}$atm and 0.61 atm.
Each curve is defined by three stages. First, for very low values of $P(Cl_2)$, no gas is formed. At this conditions $VCl_2(l)$ is present in equilibrium with graphite. The equilibrium ensemble does not experience any modification until a critical $P(Cl_2)$ value is reached, at which a discontinuity can be evidenced. The gas phase appears in equilibrium and for any $P(Cl_2)$ higher than the critical one, the number of moles $VCl_2(l)$ becomes equal to zero. This condition defines the second stage, where for higher $P(Cl_2)$ values the gas composition changes accordingly, through forming of chlorides and oxychlorides. Finally, a $P(Cl_2)$ value is reached, where all capacity of the system for forming chlorinated compounds is exhausted, and the effect of adding more Cl_2 is only the dilution of the chlorinated species formed. As a consequence, the number of mole of gas phase experiences a significant elevation. At 1073 K, for example, Figure (26) describes the effect of $P(Cl_2)$ over the gas phase composition during the second and third stages. We see that the mol fraction of VCl_4 raises (second stage) and after achieving a maximum value starts to decrease (third stage). The concentration variations during the second sage can be ascribed to the occurrence of reactions represented by Eq. (48), which have at 1073 K equilibrium constants much higher than unity (Table 3). The reduction of the mol fraction of $VOCl_3$ can be understood as a dilution effect, which is motivated by the elevation of the mol fractions of VCl_4 and Cl_2.

$$\begin{aligned} VCl_2 + Cl_2 &\rightarrow VCl_4 \\ VCl_3 + 0.5Cl_2 &\rightarrow VCl_4 \end{aligned} \tag{48}$$

K	Chemical reaction
$1.95.10^5$	$VCl_2 + Cl_2 \rightarrow VCl_4$
$2.12.10^3$	$VCl_3 + 0.5Cl_2 \rightarrow VCl_4$

Table 3. Equilibrium constants at 1073 K for the reactions represented by Eq. (48)

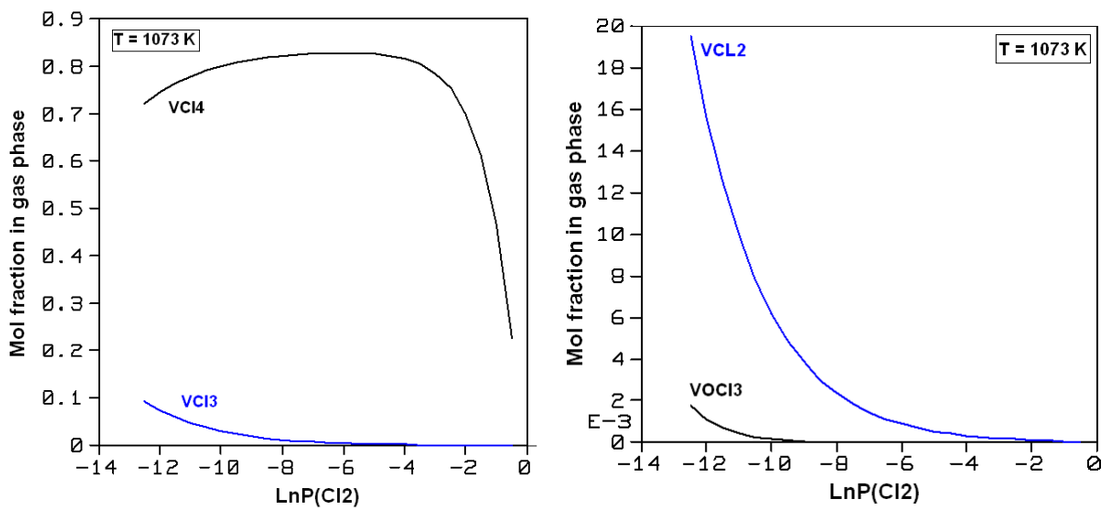

Fig. 26. Concentration of vanadium chlorides and oxychlorides as a function of $P(Cl_2)$ at 1073 K

Besides $P(Cl_2)$, temperature should also have an effect over the composition of the gas phase. This was studied as follows. Six temperature values were chosen in the range between 1073 K and 1473 K. Next, for each temperature the critical $P(Cl_2)$ value (the one associated with the formation of the first gas molecules) is identified. The composition of the most stable gaseous species is then computed and is presented in Table (4). During the calculations the partial pressure of O_2 was fixed at $1.93.10^{-22}$atm.

T(K)	X(CO)	X(CO_2)	X($VOCl_3$)	X(VCl_2)	X(VCl_3)	X(VCl_4)
1073	0.16	$3.64.10^{-3}$	$1.95.10^{-2}$	$1.74.10^{-3}$	$9.27.10^{-2}$	0.72
1100	0.12	$1.23.10^{-3}$	$1.02.10^{-2}$	$2.61.10^{-3}$	0.12	0.75
1200	$4.21.10^{-2}$	$3.36.10^{-5}$	$1.08.10^{-3}$	$9.87.10^{-3}$	0.26	0.69
1300	$1.76.10^{-2}$	$1.60.10^{-6}$	$1.45.10^{-4}$	$2.98.10^{-2}$	0.43	0.52
1373	$1.00.10^{-2}$	$2.29.10^{-7}$	$3.69.10^{-5}$	$5.97.10^{-2}$	0.56	0.37
1400	$8.26.10^{-3}$	$1.17.10^{-7}$	$2.27.10^{-5}$	$7.6.10^{-2}$	0.59	0.32
1473	$5.07.10^{-3}$	$2.18.10^{-8}$	$6.22.10^{-6}$	0.14	0.66	0.19

Table 4. Composition of the "first" gas formed as a function of temperature

As expected, the mol fraction of CO is greater than the mol fraction of CO_2 for the entire temperature range studied. Also, the chloride VCl_4 has the highest concentration at 1073 K, a phase which occupies a large area of the predominance diagram at this temperature (Figure 14). As temperature attains higher values, the mol fraction of VCl_4 and $VOCl_3$ become progressive lower and the atmosphere more concentrated in VCl_2 and VCl_3. So, at 1473 K the situation is significant different from the equilibrium state observed at 1073 K. Such behavior is again consistent with the information contained on the predominance diagrams (Figures 14, 15 and 16) where can be seen that the stability fields of VCl_4(g) and $VOCl_3$(g) shrink while the area representing the phase VCl_3(g) grows. At 1573 K it occupies a visible amount of the diagrams space (Figure 16).

It is worthwhile to mention that a more detailed look on the results seems to incorporate apparent inconsistencies. i) The minimum partial pressure of Cl_2 for the formation of pure VCl_4(g) at 1073 K (Figure 14) is higher than the critical pressure for the formation of the first gaseous species at this temperature (Figure 25). ii) Measurable amounts of VCl_3 (greater or equal to 0.1) were detected for temperatures higher than 1100 K (Table 3) but no VCl_3(g) field was observed in the predominance diagram computed at 1273 K (Figure 15). iii) Also, no field associated with the formation of VCl_2(g) could be detected even at 1573 K (Figure 16) but the speciation computation predicts its presence in measurable amounts at the last temperature (x(VCl_2) = 0.14) (Table 3). All these thermodynamic values differences are a consequence of the fact that the pure molar Gibbs energy of each component is higher than its chemical potential in the ideal gas solution, the former model being used for the predominance diagrams construction while the later is applied to the speciation calculations. Therefore, the driving force for the formation of the gaseous compounds is reduced accordingly to Eq. (49).

$$\mu^{g}_{VCl_3} - g^{g}_{VCl_3} = RT \ln x^{g}_{VCl_2} < 0 \tag{49}$$

Another possible type of computation is to study the effect of $P(O_2)$ over the composition of the gas phase. This variable is restricted by the fact that the amount of graphite phase is fixed. So there is a maximum value of $P(O_2)$ at each temperature for which the

thermodynamic modeling remains consistent and the computation can be performed. By fixing the temperature at 1373K, the upper limit for $P(O_2)$ was equal to to $1.56.10^{-18}$atm and the value of $P(Cl_2)$ associated with the appearance of the first gaseous molecules is identified as $2.05.10^{-4}$atm. The composition of the gas is then computed by fixing $P(Cl_2)$ at $2.05.10^{-4}$atm. Three different $P(O_2)$ levels were studied, $1.3.10^{-24}$, $5.4.10^{-22}$ and $1.56.10^{-18}$atm. The results are presented on Table (5).

$P(O_2)$(atm)	X(CO)	$X(CO_2)$	$X(VOCl_3)$	$X(VCl_2)$	$X(VCl_3)$	$X(VCl_4)$
$1.30.10^{-24}$	$8.22.10^{-4}$	$1.54.10^{-9}$	$3.05.10^{-6}$	0.0597	0.56	0.38
$5.24.10^{-22}$	$1.65.10^{-2}$	$6.22.10^{-7}$	$6.03.10^{-5}$	0.0588	0.55	0.37
$1.56.10^{-18}$	0.902	$1.85.10^{-3}$	$3.21.10^{-4}$	$5.72.10^{-3}$	0.054	0.036

Table 5. Gas phase speciation as function of $P(O_2)$

The mol fractions of CO and CO_2 gets higher for higher values of $P(O_2)$. This is consistent with the dislocation of the equilibrium represented by Eq. (50) in the direction of the formation of the two carbon oxides.

$$\begin{aligned} C + O_2 &\rightarrow CO_2 \\ 2C + O_2 &\rightarrow 2CO \end{aligned} \tag{50}$$

Also, the Boudouard equilibrium demands that at the chosen temperature (1373 K) the atmosphere is more concentrated in CO. This was indeed observed for each equilibrium state investigated. It is interesting to observe that for $P(O_2)$ varying between $5.24.10^{-22}$atm and $1.56.10^{-18}$atm the mol fraction of CO and CO_2 experience a much higher variation in comparison with the one observed for lower $P(O_2)$ values.

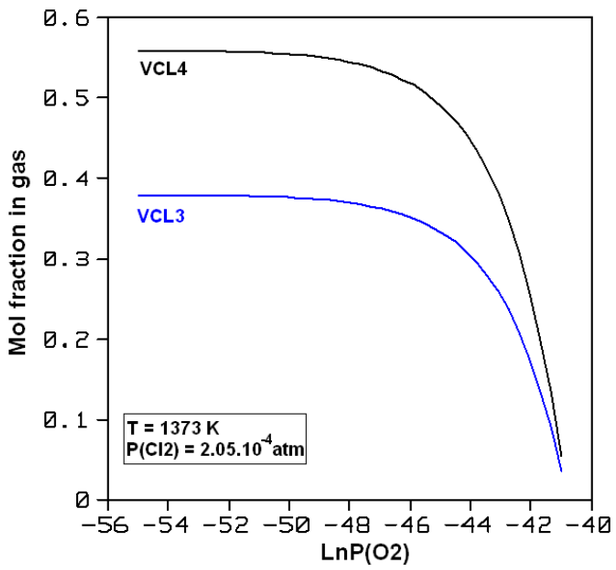

Fig. 27. Mol fractions of VCl_3 and VCl_4 as a function of $P(O_2)$

In the case of the vanadium chlorides and oxychlorides an interesting trend is evidenced. The concentration of $VOCl_3$ grows and of VCl_2, VCl_3 and VCl_4 reduce appreciably for the same O_2

partial pressure range. The concentration variations associated with the vanadium chlorinated compounds is analogous to the variations observed in the concentrations of CO and CO_2.

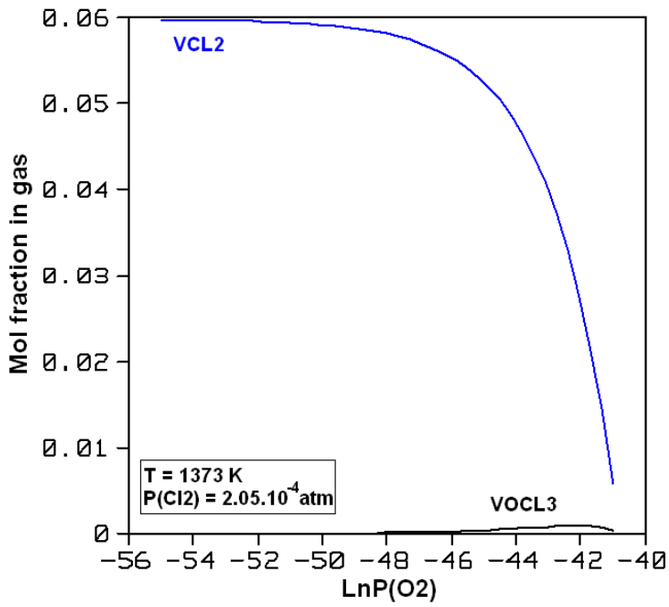

Fig. 28. Mol fractions of $VOCl_3$ and VCl_2 as a function $P(O_2)$

For $P(O_2)$ lower than $5.24.10^{-22}$atm the variations are much less significant. To get a better picture of the trend observed for the chlorides and oxychlorides, their concentrations were plotted as a function of $P(O_2)$, which was varied in the range spanned by the data of Table (5) (Figures 27, 28 and 29)

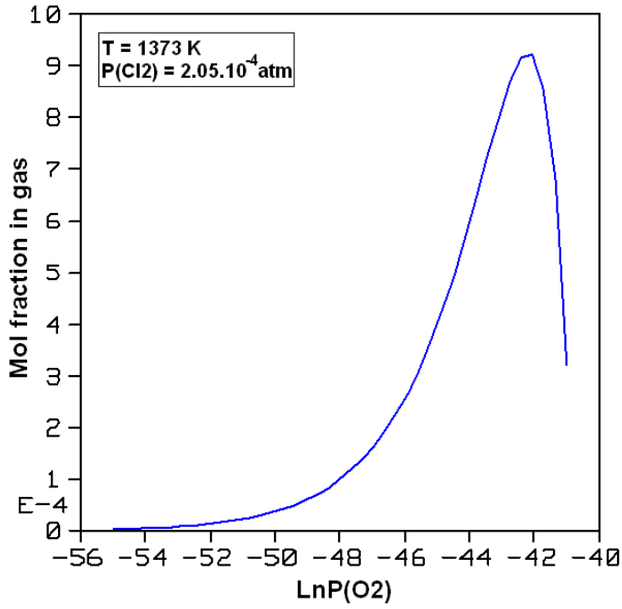

Fig. 29. Mol fraction of $VOCl_3$ as a function of $P(O_2)$

The variations depicted on Figures (27), (28) and (29) are consistent with the occurrence of reactions represented by Eq. (51). As $P(O_2)$ achieves higher values, it reacts with VCl_3, VCl_2 and or VCl_4 resulting in $VOCl_3$. Such phenomena could explain the significant reduction of VCl_3, VCl_4 and VCl_2 concentrations, and the concomitant elevation of the $VOCl_3$ mol fraction.

$$\begin{aligned} VCl_3 + 0.5O_2 &= VOCl_3 \\ VCl_2 + O_2 + VCl_4 &= 2VOCl_3 \\ VCl_4 + 0.5O_2 &= VOCl_3 + 0.5Cl_2 \end{aligned} \quad (51)$$

The participation of VCl_4 in the second reaction is supported by the fact that its equilibrium concentration lowering is more sensible to $LnP(O_2)$ than observed for VCl_3 (Figure 27). The consumption of VCl_4 by the second reaction is also consistent with the maximum observed in the curve obtained for $VOCl_3$ concentration (Figure 29). As less VCl_4 is available, less $VOCl_3$ can be produced.

K	Chemical reaction
$8.01.10^6$	$VCl_3 + 0.5O_2 = VOCl_3$
$1.89.10^{13}$	$VCl_2 + O_2 + VCl_4 = 2VOCl_3$
$1.01.10^5$	$VCl_4 + 0.5O_2 = VOCl_3 + 0.5Cl_2$

Table 6. Equilibrium constants at 1373 K for reactions represented by Eq. (51)

The occurrence of reactions represented by Eq. (51) is supported by classical thermodynamics, as the equilibrium constant (K) computed at 1373 K for all chemical reactions above assume values appreciably greater than unity (see Table 6).

3.1.3.3 V2O5 chlorination enthalpy

For the implementation of an industry process based on chemical reaction is fundamental to know the amount of heat generated or absorbed from that. Exothermic processes (heat is released) reach higher temperatures, and frequently demand engineering solutions for protecting the oven structure against the tremendous heat generated by the chemical phenomena. In this context, endothermic processes (heat is absorbed) are easier controlled, but the energy necessary to stimulate the reaction must be continuously supplied, making the energy investment larger.

The variation of the total enthalpy of the system for the chlorination process in question was calculated as a function of $P(Cl_2)$ (Figure 30). The partial pressure of O_2 was forced to be equal to $1.93.10^{-22}$atm and four temperature levels were studied, 1000 K, 1100 K, 1300 K and 1700 K. It can be seen that the total enthalpy for the process conducted at 1000 K reduces with the advent of the chlorination reactions, indicating that the chlorination process is exothermic. However, the molar enthalpy magnitude is progressively lower up to a certain temperature where it is zero. Above that, the molar reaction enthalpy becomes positive, and Figure (30) illustrates its value for 1700 K.

This is perfectly consistent with the results presented on Table (3). As temperature gets higher, the mol fractions of VCl_4 and $VOCl_3$ reduce and that for VCl_3 and VCl_2 experience a significant elevation. For some temperature between 1300 K and 1373 K the mol fractions of VCl_4 and VCl_3 assume equal values. This point is related to the condition where the chlorination enthalpy is zero. For higher temperatures, where $x(VCl_4) < x(VCl_3)$ the process

becomes progressively more endothermic. It is interesting to see that he explained behavior is consistent with the fact that the global formation reactions of VCl_3 and VCl_2 are associated with positive molar reaction enthalpies and that of $VOCl_3$ and VCl_4 with negative molar reactions enthalpies (Figure 31).

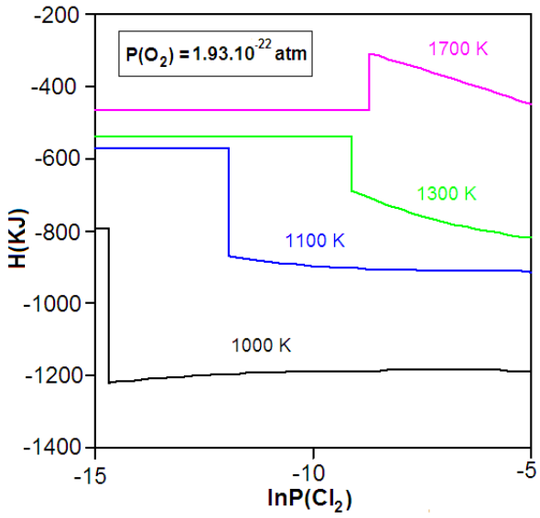

Fig. 30. Total as a function of $P(Cl_2)$

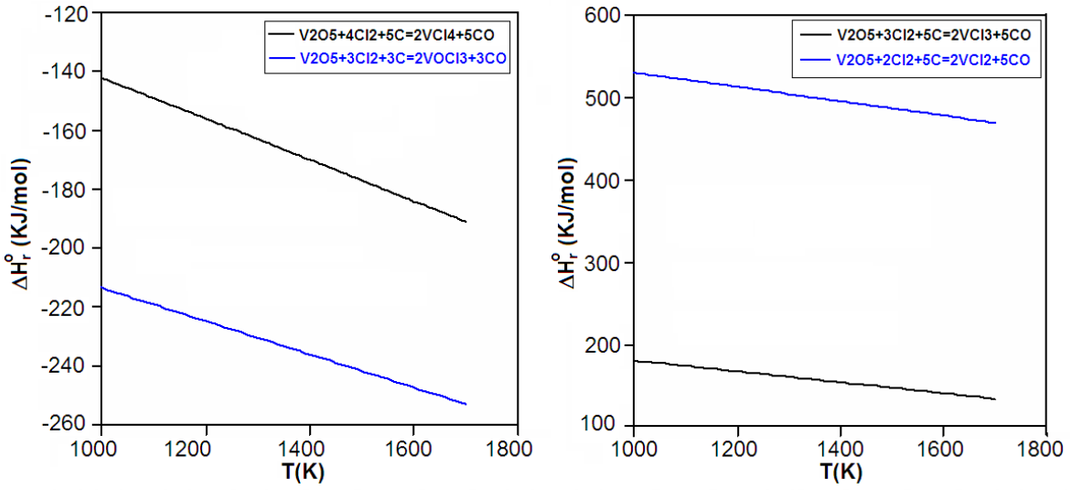

Fig. 31. Molar reaction enthalpy for the formation of gaseous VCl_3, VCl_2, VCl_4 and $VOCl_3$ as a function of temperature

4. Final remarks

In this chapter three different approaches to the chlorination equilibrium study of an oxide were presented. The first two are based on the construction of ΔG_r^o x T diagrams (topic 2.2.1) and on the calculations, first introduced by Kang & Zuo (1989) (topic 2.2.2), respectively. Both of them take into consideration that each chlorinated compound is produced independently. The third one has its fundamental based on the total Gibbs energy

minimization of the reaction system and the gas phase equilibrium composition is calculated considering that the formed species are produced simultaneously (topic 2.2.3).

The method based on the construction of ΔG_r^o x T was applied on topic (3.1.2) for studying the thermodynamic viability of the reaction between gaseous Cl_2 and V_2O_5. The discussion evidenced that the chlorination is thermodynamically feasible only in the presence of a reducing agent (graphite in the case of the present work) and was initially focused on the production of VCl_4 and $VOCl_3$. The same approach was employed for studying the possible mechanisms associated with the formation of VCl_4 and $VOCl_3$. According to the results (topic 3.1.2.1), the synthesis of these two compounds is subdivided in different stages, which can vary in nature, depending on the temperature range considered. In global terms though, both $VOCl_3$ and VCl_4 have molar reaction Gibbs energies of the same magnitude order. So, it was not possible to clearly identify, which one of them should be produced in greater quantities. The problem of the relative stability between $VOCl_3$ and VCl_4 was then addressed by the implementation of the method of Kang & Zuo (1989) (topic 3.1.3.1). The results indicated that VCl_4 should have a higher concentration in comparison with $VOCl_3$ in the temperature range between 1073 K and 1373 K.

It can de said that both, the method based on the ΔG_r^o x T diagrams construction as well as the Kang & Zuo method (1989), incorporate some simplifications and are very easy to implement. However, they lead to only a superficial knowledge of the true nature of the equilibrium state achievable. Thanks to the development of computational thermodynamic software, of which *Thermocalc* is a good example, more complex computations can be realized. For example, by allowing the chlorides and oxychlorides to build a gaseous solution, the minimization of the total Gibbs energy of the system results in the direct computation of the mol fraction of each chlorinated species present in the gas phase (topic 3.1.3.2). This method can be seen as an improvement of the idea put forward by Kang & Zuo (1989), in that all equilibrium equations are solved simultaneously, with the further advantage that one does not need to formulate a group of independent reactions that cover all possible chemical interactions among the components, a task that can become very complex for metals, as in case of vanadium, which can produce a family of chlorides and oxychlorides.

The conclusion that graphite strongly promotes the thermodynamic driving force necessary to chlorination and that VCl_4 should be formed preferentially in relation to $VOCl_3$ are perfectly consistent with the results based on the total Gibbs energy minimization. However, by the application of this last method it was possible to go a little further, through investigation of the effect of $P(Cl_2)$ over the chlorination enthalpy and by studying the effect of temperature, Cl_2 and O_2 partial pressures over the concentrations of vanadium chlorides and oxychlorides in the gas phase.

The predictions associated with the effect of temperature over the gas phase speciation (Table 4) indicate that the mol fractions of VCl_2 and VCl_3 grow significantly in the range between 1073 K and 1473 K and, as a result, the concentrations of $VOCl_3$, VCl_4, CO and CO_2 exhibit a significant reduction (topic 3.1.3.2). This finding agrees with the tendency depicted by the predominance diagrams constructed for the system V – O – Cl, where the $VCl_4(g)$ and $VOCl_3(g)$ fields shrink and that of $VCl_3(g)$ grows (Figures 14, 15 and 16). Also, the calculated mol fraction of CO is at all temperatures much higher than the mol fraction of CO_2, a fact that is consistent with the establishment of the Bourdouard equilibrium for temperatures higher than 973 K, where the concentrations of the two mentioned carbon oxides have the same magnitude.

The fact that the speciation computation indicates appreciable amounts of VCl_3 for temperatures higher than 1100 K and of VCl_2 for temperatures higher than 1473 K,

apparently contradicting the information contained in the predominance diagrams of Figures (15) and (16), is a mere consequence of the fact that on topic (3.1.3.2) the gaseous chlorides build an ideal gas solution. The chemical potentials of VCl_3 and also of VCl_2 are lower than their pure molar Gibbs energies. The species become more stable in the gaseous solution in relation to the pure state, and their mol fractions assume higher values for the same temperature imposed. The same idea explains why VCl_4 is formed in significant amounts at 1073 K for a $P(Cl_2)$ value lower than the one observed in the predominance diagram of Figure (14) for the equilibrium between $VCl_2(l)$ and $VCl_4(g)$.

The effect of adding more Cl_2 after all vanadium has been converted to gaseous chlorinated compounds is also consistent with the expectations. At 1073 K the results indicate that the mol fraction of VCl_4 grows while all other relevant chlorinated species reduces (topic 3.1.3.2). This can be explained by the reaction of VCl_2 and VCl_3 with Cl_2 resulting in VCl_4, which have a significant negative driving force at 1073 K (Table 3).

The study of the impact of varying $P(O_2)$ over the gas phase composition at 1373 K indicated that the mol fractions of CO and CO_2 experience significant elevation as $P(O_2)$ becomes higher, a fact that is also observed in the case of $VOCl_3$ (Table 4). The concentration of all other chlorinated compounds reduces for the same studied range of $P(O_2)$. The influence of the oxygen chemical activity over the gas phase speciation can be explained by a group of proposed reactions between VCl_4, VCl_3 and VCl_2 with O_2 resulting in $VOCl_3$ (topic 3.1.3.2). All these reactions have equilibrium constants much higher than one, indicating an expressive thermodynamic driving force at 1373 K (Table 6).

The conclusions about the exothermic nature of the chlorination process in the temperature range between 1000 K and 1300 K and the observation that it becomes progressively more endothermic as 1700 K is approached (topic 3.1.3.3), are perfectly consistent with the fact that the atmosphere becomes progressively diluted in VCl_4 and $VOCl_3$, whose formations are associated with negative molar enthalpies and becomes richer in VCl_2 and VCl_3, whose molar enthalpy of formation are considerably positive (Figure 31).

Finally, we can conclude that the study of the equilibrium states achievable through the reaction between a transition metal oxide and gaseous Cl_2, can be now approached through the implementation of methods of different complexity levels. The most general one, in which the total Gibbs energy of the reaction system is minimized, enables the construction of a more detailed picture of the equilibrium state. However, as it is evident from the comparisons explained above, the most general method must be consistent with the tendencies predicted by simpler calculations.

5. References

Allain E., Djona M., Gaballah I. Kinetics of Chlorination and Carbochlorination of Pure Tantalum and Niobium Pentoxides. Metallurgical and materials transactions B, v. 28, p. 223 - 232, 1997.

Brewer L., Ebinghaus, B. B. The thermodynamics of the solid oxides of vanadium. Thermochimica Acta, v. 129, p. 49 – 55, 1988.

Brocchi, E. A.; Moura, F. J. Chlorination methods applied to recover refractory metals from tin slags. Minerals Engineering, v. 21, n. 2, p. 150-156, 2008.

Cecchi, E. et al. A feasibility study of carbochlorination of chrysotile tailings. International Journal of Mineral Processing, v. 93, n. 3 - 4, p. 278-283, 2009.

Esquivel, M. R., Bohé, A. E., Pasquevich, D. M. Carbochlorination of samarium sesquioxide. Thermoquimica Acta, v. 403, p. 207 – 218, 2003.

Gaballah, I., Djona, M. Recovery of Co, Ni, Mo, and V from unroasted spent hydrorefining catalysts by selective chlorination. Metallurgical and Materials Transactions B, v. 26, n. 1, p. 41-50, 1995.

Gaviria, J. P., Bohe, A. E. Carbochlorination of yttrium oxide. Thermochimica Acta, v. 509, n. 1-2, p. 100-110, 2010.

Gonzallez J. et al. ß-Ta_2O_5 Carbochlorination with different types of carbon. Canadian Metallurgical Quarterly, v. 41, n.1, p. 29 - 40, 2002.

Hackert A., Plies V. and Gruehn R. Nachweis und thermochemische Charakterisierung des Gasphasenmolekuls VOCl. Zeitschrift für anorganische und allgemeine Chemie, v. 622, p. 1651-1657, 1996.

Hildenbrand, D. L. et al. Thermochemistry of the Gaseous Vanadium Chlorides VCl, VCl_2, VCl_3, and VCl_4. Journal of Physical Chemistry A, v. 112, p. 9978 – 9982, 2008.

Jena, P. K.; Brocchi, E. A.; Gonzalez, J. Kinetics of low-temperature chlorination of vanadium pentoxide by carbon tetrachloride vapor. Metallurgical and Materials Transactions B, v. 36, n. 2, p. 195-199, 2005.

Kang, S. X.; Zuo, Y. Z. Chloridizing roasting of complex material containing low tin and high iron at high temperature. Kunming Metall. Res. Inst. Report, v. 89, n. 3, 1989.

Kellog, H. H. Thermodynamic relationships in chlorine metallurgy. Journal of metals, v. 188, p. 862 – 872, 1950.

Mackay, D. Is chlorine the evil element? Enviromental Science & Engineering, p. 49 – 52, 1992.

McCarley R. E., Roddy J. W. The Vapor Pressures of Vanadium(II) Chloride, Vanadium(III) Chloride, Vanadium(II) Bromide, and Vanadium(III) Bromide by Knudsen Effusion. Inorganic Chemistry, v. 3. n. 1, p. 60 - 63, 1964.

Micco, G.; Bohe, A. E.; Sohn, H. Y. Intrinsic Kinetics of Chlorination of WO_3 Particles With Cl_2 Gas Between 973 K and 1223 K (700°C and 950 °C. Metallurgical and Materials Transactions B, v. 42, n. 2, p. 316-323, 2011.

Murase, K. et al. Recovery of vanadium, nickel and magnesium from a fly ash of bitumen-in-water emulsion by chlorination and chemical transport. Journal of Alloys and Compounds, v. 264, n. 1 - 2, p. 151-156, 1998.

Neff, D. V. Environmentally acceptable chlorination processes. Aluminium Cast House Technology: Theory & Practice, Australasian, Asian, Pacific Conference, p. 211-225, 1995.

Oheda, M. W., Rivarola, J. B., Quiroga, O. D. Study of the chlorination of molybdenum trioxide mixed with carbon black. Minerals Engineering, v. 15, p. 585 – 591, 2002.

Oppermann, H. Preparation and properties of VCl_4, VCl_3, and $VOCl_3$. Zeitschrift für Chemie, v. 2, p. 376 – 377, 1962.

Oppermann H. Gleichgewichte mit $VOCl_3$, VO_2Cl, und $VOCl_2$. Zeitschrift für anorganishce und algemeine Chemie, v. 331, n. 3 - 4, p. 113 - 224, 1967.

Patel, C. C., Jere, G. V. Some Thermodynamical considerations in the chlorination of Ilmetite. Transactions of the metallurgical society of AIME, v. 218, p. 219 – 225, 1960.

Pilgrim, R. F., Ingraham, T. R. Thermodynamics of chlorination of iron, cobalt, nickel and copper sulphides. Canadian Metallurgical Quarterly, v. 6, n. 4, p. 333 - 346, 1967.

Robert, T. D. Thermodynamics in materials science, 1993.

Sano N., Belton, G. The thermodynamics of chlorination of Vanadium Pentoxide. Transactions of the Japan Institute of Metals, v.21, n. 9, p. 597 – 600, 1980.

Schäffer H., Wartenpfuhl H. Über die Herstellung von VOCl. Journal of the less common metals, v. 3, p. 29 – 33, 1961.

Zhang, L. et al. Rare earth extraction from bastnaesite concentrate by stepwise carbochlorination - chemical vapor transport-oxidation. Metallurgical and Materials Transactions B, v. 35, n. 2, p. 217-221, 2004.

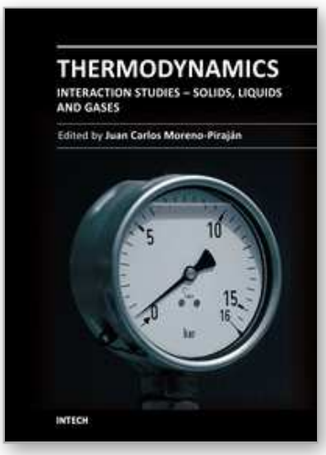

Thermodynamics - Interaction Studies - Solids, Liquids and Gases
Edited by Dr. Juan Carlos Moreno PirajÃ¡n

ISBN 978-953-307-563-1
Hard cover, 918 pages
Publisher InTech
Published online 02, November, 2011
Published in print edition November, 2011

Thermodynamics is one of the most exciting branches of physical chemistry which has greatly contributed to the modern science. Being concentrated on a wide range of applications of thermodynamics, this book gathers a series of contributions by the finest scientists in the world, gathered in an orderly manner. It can be used in post-graduate courses for students and as a reference book, as it is written in a language pleasing to the reader. It can also serve as a reference material for researchers to whom the thermodynamics is one of the area of interest.

How to reference
In order to correctly reference this scholarly work, feel free to copy and paste the following:

Brocchi E. A. and Navarro R. C. S. (2011). On the Chlorination Thermodynamics, Thermodynamics - Interaction Studies - Solids, Liquids and Gases, Dr. Juan Carlos Moreno PirajÃ¡n (Ed.), ISBN: 978-953-307-563-1, InTech, Available from: http://www.intechopen.com/books/thermodynamics-interaction-studies-solids-liquids-and-gases/on-the-chlorination-thermodynamics

INTECH
open science | open minds

InTech Europe
University Campus STeP Ri
Slavka Krautzeka 83/A
51000 Rijeka, Croatia
Phone: +385 (51) 770 447
Fax: +385 (51) 686 166
www.intechopen.com

InTech China
Unit 405, Office Block, Hotel Equatorial Shanghai
No.65, Yan An Road (West), Shanghai, 200040, China
中国上海市延安西路65号上海国际贵都大饭店办公楼405单元
Phone: +86-21-62489820
Fax: +86-21-62489821

IntechOpen